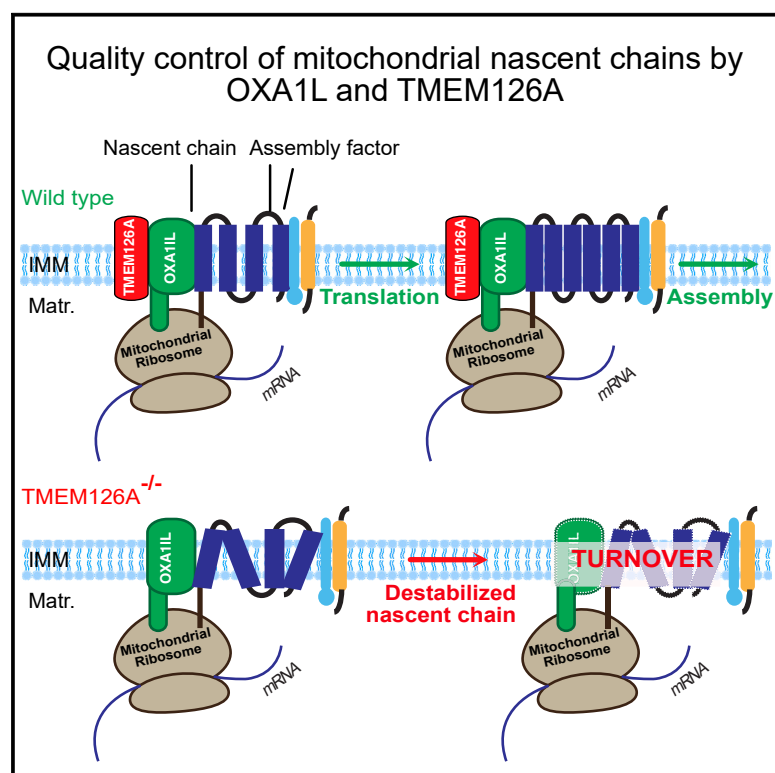


# Identification of TMEM126A as OXA1L-interacting protein reveals cotranslational quality control in mitochondria

## Graphical abstract



## Authors

Sabine Poerschke, Silke Oeljeklaus, Luis Daniel Cruz-Zaragoza, ..., Bettina Warscheid, Sven Dennerlein, Peter Rehling

## Correspondence

sven.dennerlein@med.uni-goettingen.de (S.D.),  
peter.rehling@medizin.uni-goettingen.de (P.R.)

## In brief

Poerschke et al. define TMEM126 as a protein that forms a complex with the OXA1L insertase in mitochondria to facilitate membrane insertion of mitochondrial-encoded polypeptides. Loss of TMEM126 triggers turnover of OXA1L insertase and its accumulated cargo by the inner membrane quality control system.

## Highlights

- Human mitochondrial OXA1L interacts with TMEM126A in a translational-independent manner
- Both proteins are required for mitochondrial-encoded protein biogenesis
- Defective protein insertion triggers turnover of nascent chains and OXA1L insertase



## Article

# Identification of TMEM126A as OXA1L-interacting protein reveals cotranslational quality control in mitochondria

Sabine Poerschke,<sup>1</sup> Silke Oeljeklaus,<sup>2</sup> Luis Daniel Cruz-Zaragoza,<sup>1</sup> Alexander Schendzielorz,<sup>3</sup> Drishan Dahal,<sup>1</sup> Hauke Sven Hillen,<sup>1,4,5</sup> Hirak Das,<sup>2</sup> Laura Sophie Kremer,<sup>1</sup> Anusha Valpadashi,<sup>1</sup> Mirjam Breuer,<sup>1</sup> Johannes Sattmann,<sup>1</sup> Ricarda Richter-Dennerlein,<sup>1,4,6</sup> Bettina Warscheid,<sup>2,7</sup> Sven Dennerlein,<sup>1,\*</sup> and Peter Rehling<sup>1,4,6,8,9,10,\*</sup>

<sup>1</sup>Institute for Cellular Biochemistry, University of Goettingen, 37073 Goettingen, Germany

<sup>2</sup>Faculty of Chemistry and Pharmacy, Biochemistry II, Theodor Boveri-Institute, University of Würzburg, 97074 Würzburg, Germany

<sup>3</sup>Institute for Biology II, Faculty for Biology, Functional Proteomics, University of Freiburg, 79104 Freiburg, Germany

<sup>4</sup>Cluster of Excellence “Multiscale Bioimaging: from Molecular Machines to Networks of Excitable Cells” (MBExC), University of Goettingen, Goettingen, Germany

<sup>5</sup>Research Group Structure and Function of Molecular Machines, Max Planck Institute for Multidisciplinary Sciences, 37077 Goettingen, Germany

<sup>6</sup>Goettingen Center for Molecular Biosciences, University of Goettingen, 37077 Goettingen, Germany

<sup>7</sup>Cluster of Excellence CIBSS Centre for Integrative Biological Signalling Studies, University of Freiburg, 79104 Freiburg, Germany

<sup>8</sup>Fraunhofer Institute for Translational Medicine and Pharmacology ITMP, Translational Neuroinflammation and Automated Microscopy, Goettingen, Germany

<sup>9</sup>Max Planck Institute for Multidisciplinary Sciences, 37077 Goettingen, Germany

<sup>10</sup>Lead contact

\*Correspondence: [sven.dennerlein@med.uni-goettingen.de](mailto:sven.dennerlein@med.uni-goettingen.de) (S.D.), [peter.rehling@medizin.uni-goettingen.de](mailto:peter.rehling@medizin.uni-goettingen.de) (P.R.)

<https://doi.org/10.1016/j.molcel.2023.12.013>

## SUMMARY

Cellular proteostasis requires transport of polypeptides across membranes. Although defective transport processes trigger cytosolic rescue and quality control mechanisms that clear translocases and membranes from unproductive cargo, proteins that are synthesized within mitochondria are not accessible to these mechanisms. Mitochondrial-encoded proteins are inserted cotranslationally into the inner membrane by the conserved insertase OXA1L. Here, we identify TMEM126A as a OXA1L-interacting protein. TMEM126A associates with mitochondrial ribosomes and translation products. Loss of TMEM126A leads to the destabilization of mitochondrial translation products, triggering an inner membrane quality control process, in which newly synthesized proteins are degraded by the mitochondrial iAAA protease. Our data reveal that TMEM126A cooperates with OXA1L in protein insertion into the membrane. Upon loss of TMEM126A, the cargo-blocked OXA1L insertase complexes undergo proteolytic clearance by the iAAA protease machinery together with its cargo.

## INTRODUCTION

Expression of the mitochondrial genome is essential for the biogenesis of the oxidative phosphorylation system (OXPHOS) in the inner membrane. The human mitochondrial DNA (mtDNA) encodes 13 polypeptides that are inner membrane proteins and core components of the OXPHOS system. The respiratory chain complexes (I, III, and IV) and the ATP synthase (V) are built of mitochondrial- and nuclear-encoded subunits.<sup>1–6</sup> Accordingly, imported subunits of the complexes have to associate with the membrane-embedded mitochondrial-encoded partner proteins to form the active enzyme complexes. The import into mitochondria is facilitated by the translocase of the outer mitochondrial membrane (TOM complex) and dedicated TIM (translocase of the inner mitochondrial membrane) complexes, which mediate inner mem-

brane passage of the imported polypeptides across and into the inner membrane. The insertion of mitochondrial-encoded proteins into the inner membrane is mediated by the OXA1 insertase.

OXA1 is a member of the Oxa1/YidC/Alb3 protein family that is evolutionarily related to the ER membrane complex (EMC).<sup>7–9</sup> Metazoan OXA1L and its counterparts in lower eukaryotes (Oxa1)<sup>9,10</sup> span the inner membrane five times. The C-terminal domain of the protein is exposed to the mitochondrial matrix and provides the platform for binding to the mitochondrial ribosome.<sup>11–14</sup> Through this interaction, Oxa1 facilitates the cotranslational insertion of mitochondrial translation products into the lipid phase.<sup>15–17</sup> Moreover, membrane insertion of a subset of nuclear-encoded membrane proteins depends on the OXA pathway.<sup>18–20</sup>

Most studies on Oxa1 have been carried out in the yeast *Saccharomyces cerevisiae*, but the human OXA1L-insertase



machinery is still poorly defined. Loss of *OXA1L* in human cells was shown to affect complex I and complex IV biogenesis.<sup>21</sup> A recently identified patient with a mutation in *OXA1L*, who displayed OXPHOS deficiency with hypotonia, encephalopathy, and fatal cardiorespiratory arrest, showed reduced levels of complexes I, IV, and V and destabilization of mitochondrial translation products in isolated fibroblasts.<sup>22</sup> Moreover, structural analysis on the mitochondrial ribosome provided molecular information on the *OXA1L* ribosome association and suggested that *OXA1L* is bound to the mtLSU through interactions with mL45 and uL23m.<sup>13,23–25</sup>

Although it is commonly accepted that *OXA1L* is essential for the biogenesis of the OXPHOS machinery by acting as the key insertase for mitochondrial-encoded proteins, molecular insights into the membrane insertion process itself are still lacking. Moreover, it remains unaddressed whether *OXA1L* fulfills its functions alone or whether its function depends on the interplay with other factors within a complex. To close this gap, we defined the human *OXA1L* interactome using a variant of *OXA1L* tagged within the N-terminal portion of the protein. Here, we identified TMEM126A as an unknown interactor of the human *OXA1L*-insertase machinery. TMEM126A is quantitatively associated with *OXA1L* and mitochondrial ribosomes. TMEM126A depletion destabilizes translation products and triggers an inner mitochondrial membrane quality control process. In the absence of TMEM126A, the *OXA1L* protein is turned over by the iAAA protease together with newly synthesized mitochondrial-encoded polypeptides. Thus, our study defines an unknown interactor of the *OXA1L* insertase and identifies a mechanism of quality control to clear the inner membrane from the clogged protein insertion machinery.

## RESULTS

### Mapping constituents of the human *OXA1L* insertase

To define constituents of the human *OXA1L* complex, we generated stable HEK293 cell lines, expressing *OXA1L* with FLAG tags inserted at different positions (Figure 1A). Previous studies used an *OXA1L* version tagged at the C terminus.<sup>22</sup> Considering that the C terminus of *OXA1L* mediates the interaction with the mitochondrial ribosome<sup>11,12,14</sup> and the observation that tagging of yeast *Oxa1* with a C-terminal tag affected ribosome association,<sup>26</sup> we designed FLAG-tagged versions of *OXA1L* in which the tag was introduced near the C terminus (after amino acid 326 or 397) or adjacent to the predicted presequence in the N-terminal region (amino acid 74) (Figure 1A). To investigate the functionality of these proteins, we purified mitochondria expressing the tagged *OXA1L* variants and subjected these to FLAG immunoprecipitation (Figure 1B). The N-terminally tagged version of *OXA1L* (<sup>FLAG</sup>*OXA1L*) efficiently purified the mitochondrial ribosome and the membrane integral early assembly factors MITRAC12 and C12ORF73 (Figure 1B, lane 6). In contrast, C-terminally tagged *OXA1L* was less efficiently purified, and only minor amounts of interacting ribosomal proteins were observed in the eluate (Figure 1B, lanes 7 and 8). Hence, an N-terminally tagged version of *OXA1L* enables efficient purification of the protein together with associated ribosomes and early assembly factors.

Based on the immunoprecipitation result, we used <sup>FLAG</sup>*OXA1L* for preparative scale purification. <sup>FLAG</sup>*OXA1L* specifically purified proteins in amounts that could be visualized by colloidal Coomassie staining (Figure 1C). To define the *OXA1L* interactome, we performed a quantitative mass spectrometric analysis of the purified complex utilizing a stable isotope labeling with amino acids in cell culture (SILAC)-based strategy (Figure 1D; Table S1). As expected, we identified proteins of the large and small mitochondrial ribosomal subunits (mtLSU:blue and mtSSU:yellow) and factors involved in respiratory chain assembly (Figure 1D; Table S1). Selected enriched proteins of the <sup>FLAG</sup>*OXA1L* immunoprecipitations were confirmed by western blot analysis (Figure 1E). Among the isolated *OXA1L*-interacting proteins, TMEM126A represented a largely functionally uncharacterized protein. Mutations in TMEM126A have been linked to optic atrophy, and a role in complex I assembly has been proposed; however, an association with *OXA1L* has not been reported.<sup>27,28</sup> Interestingly, approximately 70% of TMEM126A copurified with *OXA1L* when the endogenous *OXA1L* was immunoprecipitated with an *OXA1L* antibody (Figure 1F). The interaction of *OXA1L* and TMEM126A was furthermore confirmed by performing the reverse immunoprecipitation experiment using an antiserum directed against TMEM126A (Figure S1A). In addition to *OXA1L*, components of complex I were immunoprecipitated, which is in line with the reported involvement of TMEM126A in complex I assembly.<sup>28,29</sup> Similar to *OXA1L*, TMEM126A represents a multispanning inner membrane protein according to MitoCarta3.0.<sup>30</sup> We confirmed inner membrane localization by protease protection analysis (Figure S1B). Upon disruption of the outer membrane by hypotonic swelling, TMEM126A was accessed by the protease indicating that its N and C termini face the mitochondrial intermembrane space (Figures S1B and S1C).

Considering the interaction of *OXA1L* with the mitochondrial ribosome, we tested whether TMEM126A also displayed ribosome association. Therefore, purified mitochondria from mL62<sup>FLAG</sup>-expressing cells were subjected to immunoprecipitation experiments, and eluates were analyzed by western blotting. In addition to *OXA1L*, TMEM126A was efficiently co-immunoprecipitated with the mitochondrial ribosome (Figure 1G). This was further confirmed by mass spectrometric analyses of immunoprecipitations using an antiserum directed against the endogenous TMEM126A (Table S2). In summary, although previous studies suggested that TMEM126A facilitates complex I biogenesis, we observed here that the protein associates with the mitochondrial ribosome and the *OXA1L*-insertase machinery.

### TMEM126A-*OXA1L* interaction is translation independent

To define the requirements for the association between TMEM126A and *OXA1L*, we inhibited mitochondrial translation with thiamphenicol (TAP) in <sup>FLAG</sup>*OXA1L*-expressing cells. Subsequently, mitochondria were subjected to FLAG immunoprecipitation. Interestingly, mitochondrial translation activity was not required for the association of *OXA1L* with ribosomes or TMEM126A, since <sup>FLAG</sup>*OXA1L* copurified equal amounts of mitochondrial ribosomes (mL45, uL23m, mL62, uS14m, and mS39) and TMEM126A independent of TAP treatment (Figure 2A). To further investigate if the interaction of TMEM126A with the mitochondrial ribosome

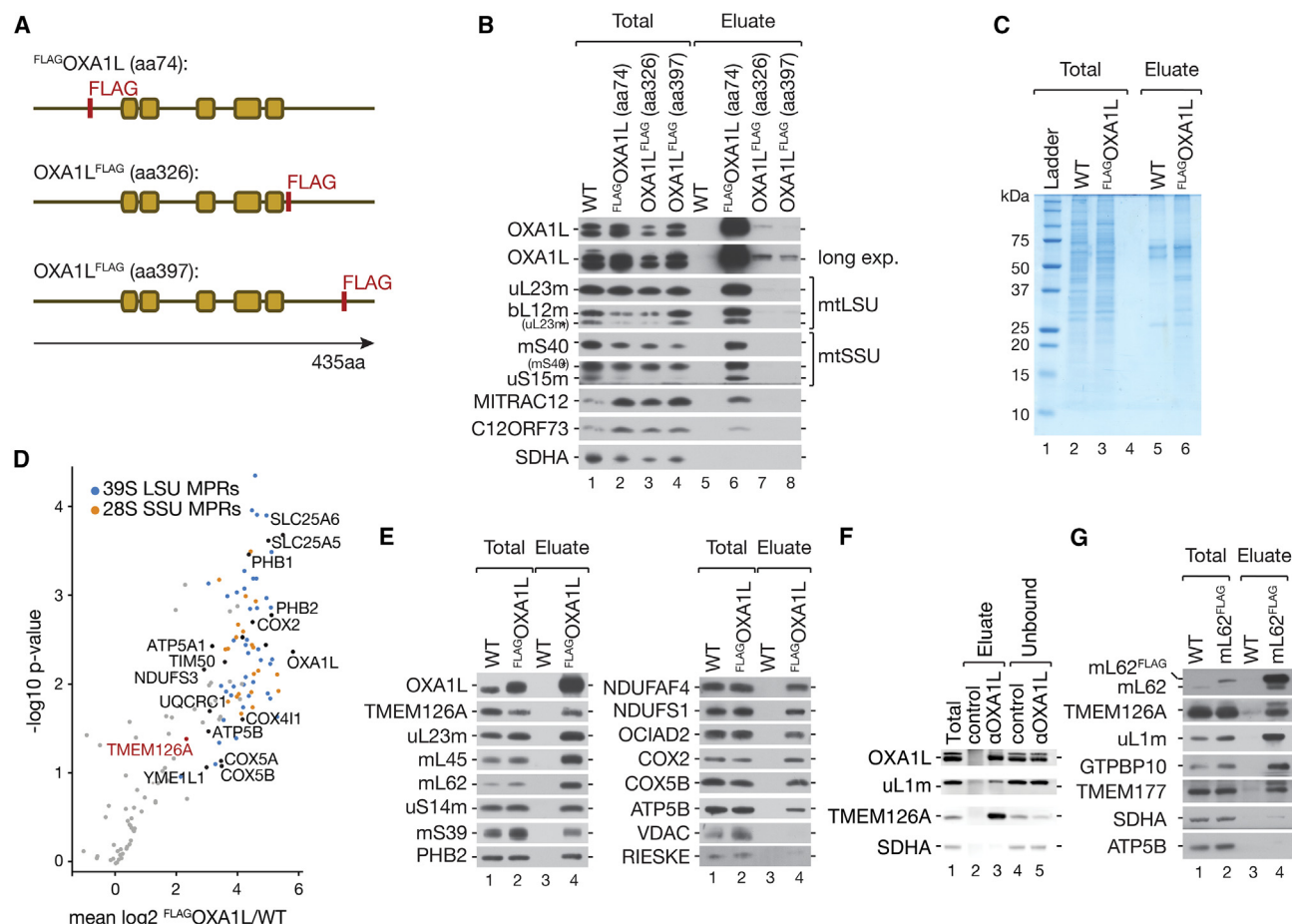


**Figure 1. TMEM126A is an interactor of OXA1L**

(A) Schematic presentation of OXA1L<sup>FLAG</sup> constructs used in this study. FLAG-tag was inserted after amino acid 74, 326, or 397.

(B) Mitochondria isolated from HEK293 cells expressing indicated FLAG-tagged OXA1L versions and wild-type (WT) control were isolated and subjected to immunoprecipitations. Eluates were subjected to western blotting; total 2%, eluate 100%.

(C) Mitochondria from wild-type (WT) and FLAG-OXA1L-expressing HEK293 cells were solubilized with subjected to immunoprecipitation. Eluates (100%) were analyzed by SDS-PAGE, followed by Coomassie staining.

(D) Wild-type (WT) and FLAG-OXA1L-expressing cells were cultured in SILAC-media, mitochondria isolated, subjected to anti-FLAG immunoprecipitation, and eluates analyzed by quantitative mass spectrometry (liquid chromatography-tandem mass spectrometry [LC-MS/MS]) (n = 4).

(E) Proteins identified in (D) were confirmed by western blot analysis. Antibodies were applied as indicated total 1.3%, eluate 100%.

(F) Immunoprecipitation using antiserum against the endogenous OXA1L or a control protein. Total 1%, eluates 100%.

(G) Mitochondria from wild-type (WT) and mL62<sup>FLAG</sup>-expressing cells were subjected to anti-FLAG immunoprecipitation and eluates analyzed by western blotting with indicated antibodies. Total 1%, eluates 100%.

See also Figure S1 and Tables S1 and S2.

was OXA1L dependent, we used small interfering RNA (siRNA)-mediated depletion of OXA1L (Figure S2A). Although we observed a subtle reduction of TMEM126A and TMEM126B upon siOXA1L treatment, we isolated mitochondria from these cells and performed immunoprecipitations using TMEM126A antibodies. Reproducibly, the isolation of TMEM126A after siRNA-mediated reduction of OXA1L did not alter the interaction between TMEM126A and the mitochondrial ribosome (Figure S2B).

Recent structural studies suggested that OXA1L binds to the ribosome via the mL45 protein of the large subunit.<sup>23</sup> Therefore, we monitored steady-state protein levels of OXA1L and TMEM126A in mitochondria, which were depleted of the mitochondrial ribosome, using a mL45 knockout cell line (mL45<sup>-/-</sup>)

(Figure 2B). Ribosomal proteins of the mtSSU, such as uS14m, were decreased in the mL45<sup>-/-</sup> cell line. However, the steady-state protein levels of OXA1L and TMEM126A appeared slightly increased (Figure 2B). Using an antibody against OXA1L, we performed an immunoprecipitation from mitochondria isolated from wild-type (WT) and mL45<sup>-/-</sup> cells (Figure 2C). Despite the lack of mL45 and the concomitant loss of functional ribosomes, we efficiently coisolated TMEM126A together with the large subunit protein uL1m. Accordingly, ribosomal remnants are able to associate with the OXA1L insertase, which suffices to maintain the OXA1L-TMEM126A interaction. In a complementary approach to assess the interaction of OXA1L and TMEM126A in the absence of the mitochondrial ribosome, we used an established

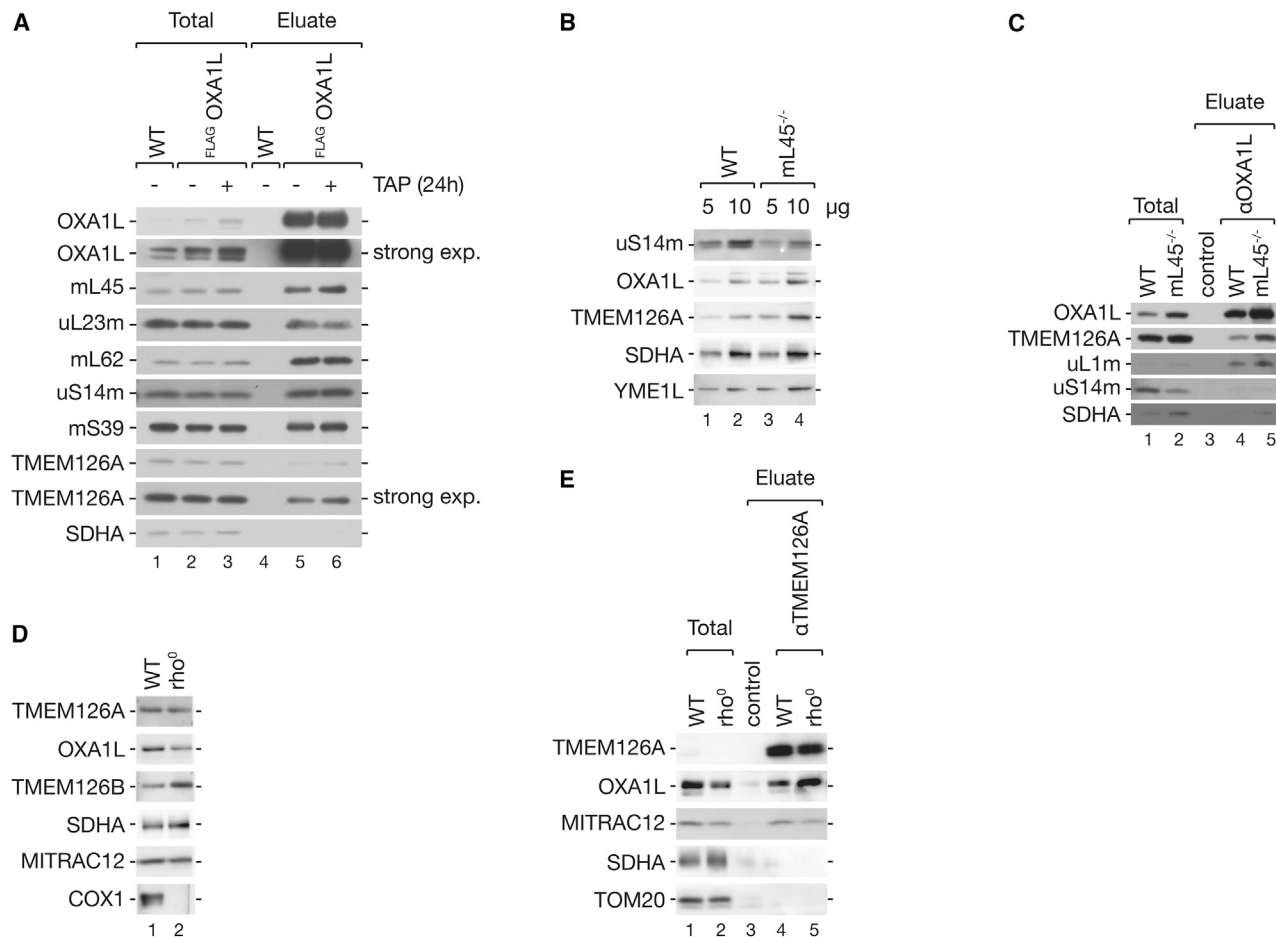


**Figure 2. TMEM126A interacts with OXA1L in a stoichiometric manner**

(A) Cells expressing FLAG-OXA1L were treated with thiamphenicol (TAP) for 24 h, prior to mitochondria isolation. Anti-FLAG immunoprecipitations were performed and eluates subjected to western blot analysis. Total 1%; eluate 100%.

(B) mL45<sup>-/-</sup> HEK293 cells were solubilized and subjected to western blot analysis, using indicated antibodies.

(C) Mitochondria from wild-type (WT) cell or cells lacking mL45 were isolated and subjected to anti-OXA1L immunoprecipitation. Eluates were analyzed by western blotting. Total 1%; eluate 100%.

(D) Western blot analysis of purified mitochondria from wild-type and rho<sup>0</sup> cells for selected mitochondrial proteins.

(E) Immunoprecipitation of endogenous TMEM126A with mitochondria from wild type or rho<sup>0</sup> cells followed by western blot analysis. Total 1%; eluate 100%.

See also Figure S2.

rho<sup>0</sup> cell line model, which lacks mtDNA. Although OXA1L levels were slightly reduced in these mitochondria, TMEM126A appeared normal (Figure 2D). Interestingly, using the TMEM126A antibody for immunoprecipitations, the association with OXA1L was not affected. Apparently, OXA1L isolated slightly more efficient compared with the WT control in the rho<sup>0</sup> sample (Figure 2E).

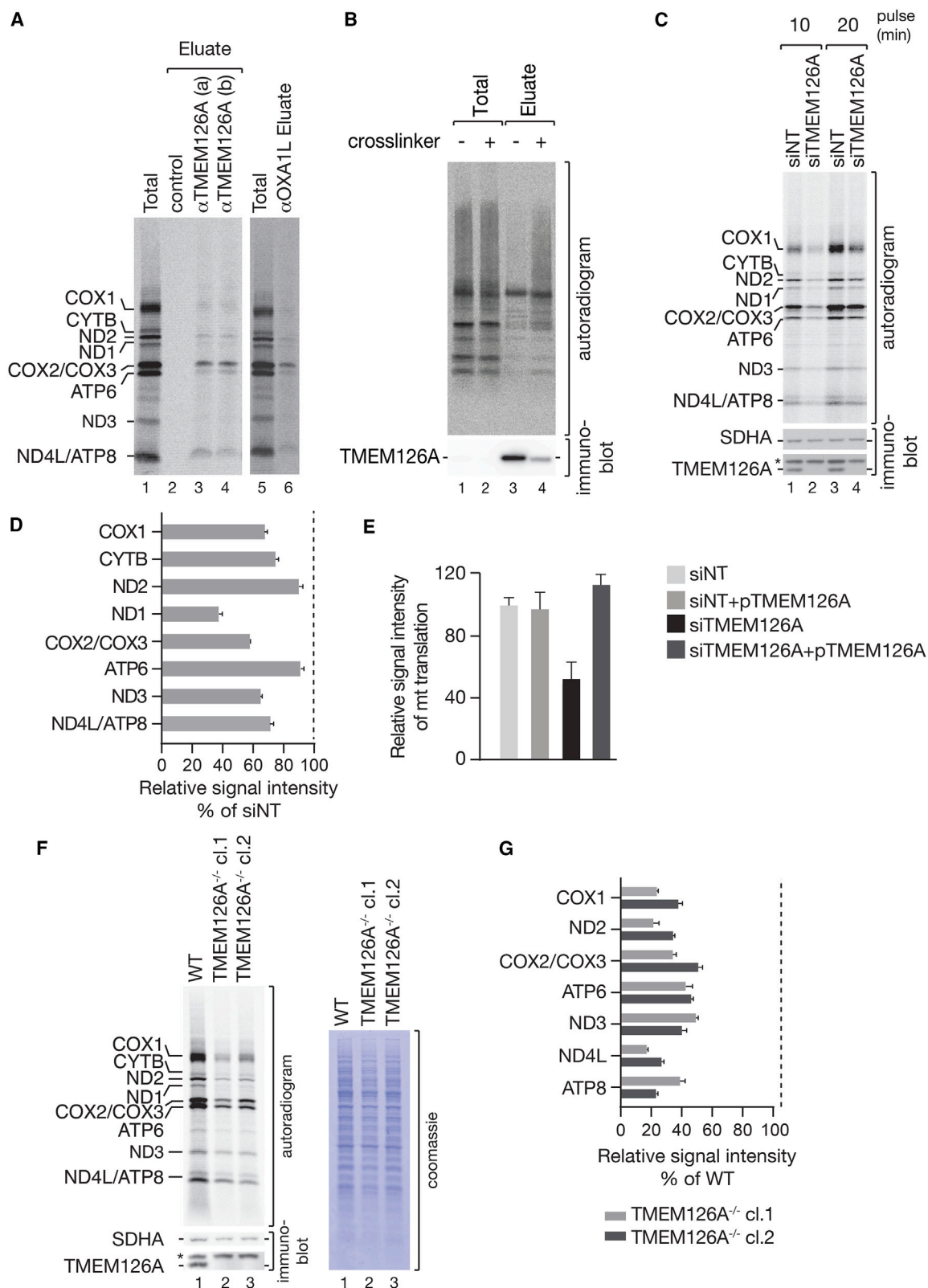
In summary, we show that TMEM126A is associated with the OXA1L-insertase complex in mitochondria and that the interaction between OXA1L and TMEM126A is independent of active mitochondrial translation or OXA1L association with the ribosome.

### TMEM126A interacts with newly synthesized translation products

Oxa1 in yeast interacts with newly synthesized mitochondrial polypeptides that are cotranslationally inserted into the inner membrane.<sup>11,14,16,31</sup> Considering that TMEM126A represents a

constituent of the OXA1L-insertase complex in humans, we addressed whether TMEM126A similarly interacted with newly synthesized mitochondrial-encoded proteins. Therefore, HEK293 cells were incubated with [<sup>35</sup>S]methionine after the inhibition of cytosolic protein synthesis. Antibodies against TMEM126A and OXA1L were used for immunoprecipitation after [<sup>35</sup>S]methionine labeling of mitochondrial translation products (Figure 3A). Indeed, newly synthesized mitochondrial translation products copurified with TMEM126A (Figure 3A, lanes 3 and 4), and the pattern of isolated translation products appeared to be similar compared with OXA1L immunoprecipitates (Figure 3A, lane 6). Since TMEM126A formed a complex with the OXA1L insertase, we tested if TMEM126A also interacted directly with newly synthesized mitochondrial-encoded proteins (Figure 3B). To this end, we used chemical cross-linking combined with immunoprecipitation under denaturing conditions to investigate this interaction.





(legend on next page)

Indeed, newly synthesized proteins coisolated with TMEM126A under these conditions.

The observed co-isolation of newly synthesized mitochondrial translation products and the interaction with OXA1L and ribosomes led us to investigate mitochondrial protein synthesis in the absence of TMEM126A. Therefore, we depleted TMEM126A by siRNA treatment and performed pulse labeling using [<sup>35</sup>S]methionine for different time points (Figure 3C). Compared with the non-targeting control, mitochondrial translation products were significantly reduced in the TMEM126A-ablated cells. The most affected translation product was ND1, which reached only 40% of the control (Figure 3D). This translation or protein stability defect was fully rescued upon re-expression of TMEM126A by transient transfection showing the specificity of the used siRNA (Figure 3E). In addition, we generated TMEM126A<sup>-/-</sup> knockout cell lines using the CRISPR-Cas9 approach. We selected two cell lines (referred to as clones 1 and 2) for further analysis. Compared with the siRNA-mediated knockdown, the loss of mitochondrial translation products was even more pronounced and general in nature in both TMEM126A<sup>-/-</sup> cell lines (Figure 3F). The overall translation was drastically reduced to less than 50% of the WT cells (Figure 3G).

### Loss of TMEM126A affects OXA1L and OXPHOS complexes

To further study the function of TMEM126A, we made use of siRNA-mediated knockdown and the TMEM126A<sup>-/-</sup> cell lines. The knockdown (siTMEM126A) affected cell growth in glucose media, reducing growth by 30% compared with the non-targeting control (Figure 4A, left panel). A similar reduction of cell growth in glucose and galactose media was observed for the knockout clone 1 of TMEM126A (TMEM126A<sup>-/-</sup>), whereas clone 2 showed a stronger growth defect in glucose media (65% of WT), which was even more pronounced on galactose media (27% of WT) (Figure 4A, middle and right panels).

Next, we investigated the steady-state levels of selected mitochondrial proteins during siRNA-mediated knockdown of TMEM126A and in the TMEM126A<sup>-/-</sup> clones (Figures 4B and 4C). Knockdown of TMEM126A led to a subtle decrease in OXA1L levels, whereas subunits of complex I (NDUFB8) were strongly affected. However, tested complex III (UQCRC2), complex IV (COX1 and COX6A), and complex V (ATP5B) proteins remained unaltered. In contrast, in mitochondria isolated from TMEM126A<sup>-/-</sup>, the steady-state levels of OXA1L appeared to be slightly increased, and tested OXPHOS structural subunits were less affected, except for complex I constituents (NDUFA5 and NDUFB10; Figure 4C).

To analyze the integrity of the OXPHOS complexes, we solubilized mitochondria in dodecylmaltoside (DDM)-containing buffer and separated protein complexes by blue native (BN)-PAGE. In agreement with the protein steady-state levels in siTMEM126A-treated cells, mitochondrial complex I displayed the strongest phenotype (Figure 4D, lanes 1–4). In addition, we detected a slight decrease in complex IV and complex V levels (Figure 4D, lanes 9–12), whereas complex II and complex III appeared not to be strongly affected by TMEM126A knockdown (Figure 4D, lanes 5–8). Complex I activity measurements confirmed the decrease in complex I upon TMEM126A knockdown (Figure S3A).

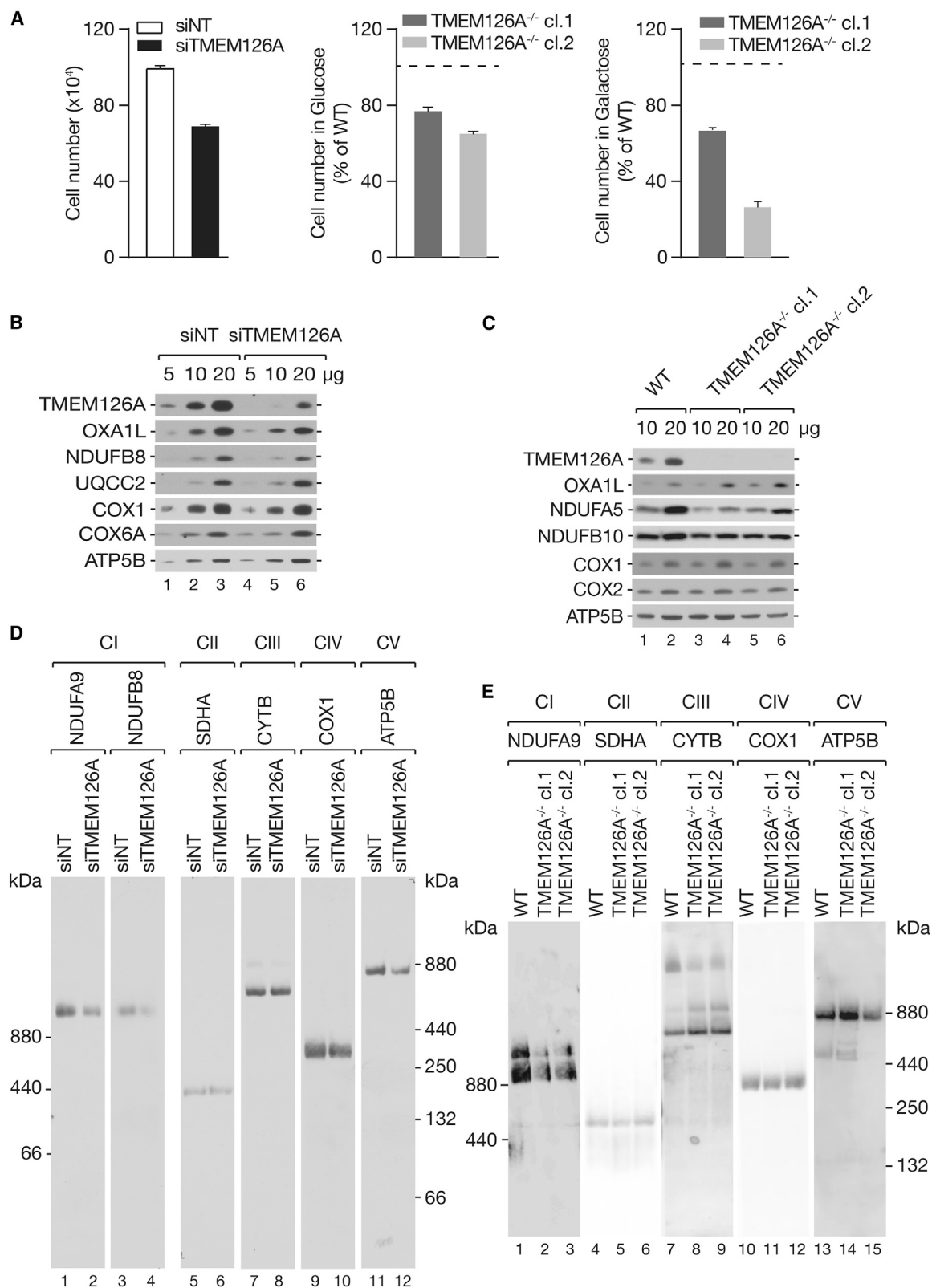
When we analyzed OXPHOS complexes in TMEM126A<sup>-/-</sup>, we observed a clear decrease in complex I amount by BN-PAGE (Figure 4E, lanes 1–3) and complex I activity by colorimetric measurements (Figure S3A). We confirmed the reduction of complex I in the TMEM126A<sup>-/-</sup> clone 1 by performing quantitative proteomic analysis of isolated mitochondria (Figure S3B; Table S3). Moreover, for TMEM126A<sup>-/-</sup> clone 2, sub-complexes of complex V, which were detected in WT and clone 1, were lacking, and assembled complex V was reduced (Figure 4E, lane 15). Both TMEM126A<sup>-/-</sup> clones appeared to be affected in complex III-containing supercomplex formation, which was detected due to incomplete dissociation by the detergent (Figure 4E, lanes 8 and 9). Using an antibody against the complex III core-subunit cytochrome b, a shift of complex III to the dimeric form was observed (Figure 4E, lanes 8 and 9). Complex II (succinate dehydrogenase complex subunit A, SDHA) and complex IV (COX1) were similar to WT (Figure 4E, lanes 4–6 and 10–12). In conclusion, loss of TMEM126A affects complex I and complex V in mitochondria. A decrease of OXA1L was apparent after acute loss of TMEM126A in the knockdown but appears to be suppressed in TMEM126A<sup>-/-</sup> cells. Considering the high selection pressure when screening for the TMEM126A<sup>-/-</sup>, it is conceivable that these cells have adapted to the metabolic challenge.

### Consecutive loss of TMEM126B leads to reduced complex I levels

The absence of TMEM126A led to decreased mitochondrial translation products. However, complex I appeared to be the most significantly affected OXPHOS complex. TMEM126A and its paralog TMEM126B were reported to both participate in the early steps of complex I assembly.<sup>28,29</sup> Interestingly, in isolated mitochondria from TMEM126A knockdown cells, we observed that the TMEM126B steady-state levels were drastically reduced compared with the non-targeting control (Figure 5A). TMEM126B was reduced to approximately 40% in the siRNA-treated

### Figure 3. Depletion of TMEM126A affects mitochondrial protein synthesis

(A) Immunoprecipitation using either TMEM126A or OXA1L antibodies from wild-type (WT) cells after radiolabeling of mitochondrial translation products. Samples were separated by SDS-PAGE and analyzed by digital autoradiography.  
(B) Radiolabeling of mitochondrial translation products during protein cross-linking, followed by immunoprecipitations of TMEM126A. Eluates were analyzed by western blots. Total 1%, eluates 100%.  
(C and D) Mitochondrial translation products were radiolabeled after siRNA-mediated depletion of TMEM126A. Whole HEK293 cell lysates were subjected to SDS-PAGE and analyses by digital autoradiography (B) and quantified (C) (SEM; n = 3).  
(E) Quantification of mitochondrial translation products after [<sup>35</sup>S]-methionine labeling of siRNA-treated cells transiently expressing TMEM126A (SEM; n = 3).  
(F) Mitochondrial translation products were radiolabeled in TMEM126A<sup>-/-</sup> cells and cell extracts analyzed by SDS-PAGE (left panel). Equal loading was confirmed by western blot and Coomassie staining (right panel).  
(G) Quantification of mitochondrial translation products as in (D) (SEM, n = 3).



(legend on next page)



cells and 25% in the TMEM126A<sup>-/-</sup> cell line (Figure S4A). We hypothesized that the complex I phenotype could be indirectly caused by the loss of TMEM126B. Therefore, we expressed untagged TMEM126B and TMEM126B<sup>FLAG</sup> in TMEM126A<sup>-/-</sup> cells. The expression of the untagged TMEM126B in TMEM126A<sup>-/-</sup> cells fully rescued the complex I defect as assessed by activity measurement and BN-PAGE (Figures 5B and 5C). However, TMEM126B<sup>FLAG</sup> was unable to complement the complex I defect (Figures 5B and 5C). Accordingly, we found that a lack of TMEM126B observed upon loss of TMEM126A causes loss of complex I. In addition, a C-terminal tag on TMEM126B renders the protein non-functional. The reduction in newly synthesized mitochondrial translation products that was apparent in TMEM126A<sup>-/-</sup> cells was not complemented by TMEM126B (Figure 5D). This observation further highlights the role of TMEM126A in mitochondrial translation or translation product stability. This was further supported, since the interaction of OXA1L and TMEM126A was not altered upon reduction of complex I levels, provoked by knockout of MTRAC15<sup>32</sup> (Figure S4B). To exclude that the reduction of mitochondrial translation products was indirectly caused by the loss of mtDNA, mtDNA levels were measured by real-time quantitative PCR (qPCR) in knockdown cells grown in either glucose- or galactose-containing media. However, no difference in the control cells was detected (Figure 5E). In agreement with this, we did not detect any significant differences in mitochondrial RNA levels measured by NanoString analysis (Figure S4C). Furthermore, steady-state levels of ribosomal subunits were assessed to address whether the reduction of newly synthesized translation products was caused by reduced amounts of mitochondrial ribosomes. However, the steady-state levels of the tested ribosomal proteins of the 39S mtLSU (uL23m and uL12m) or the 28S mtSSU (mS39 and mS40) were similar between control and knockdown cells (Figure 5F) as well as in the knockout cells (Figure 5G). Accordingly, although the complex I defect could be attributed to the loss of TMEM126B, the loss of newly synthesized translation products remained TMEM126A-specific and was not caused by DNA, RNA, or ribosome loss.

#### Quality control of the OXA1L insertase upon cargo accumulation

Considering the reduced levels of mitochondrial translation products upon loss of TMEM126A and the interaction of OXA1L with the human mitochondrial iAAA protease (Figure 1D), we investigated the stability of OXA1L in TMEM126A<sup>-/-</sup> cells. To this end, we analyzed cell lysates of WT and TMEM126A<sup>-/-</sup> cells by western blotting. Two OXA1L fragments were detected in the TMEM126A<sup>-/-</sup> cells (Figure 6A). Due to the difficult detection of these fragments in cells, we carried out further experiments in iso-

lated mitochondria under translation-enabling conditions, since purified mitochondria are capable of translating their mRNAs, allowing for biochemical dissection of translation-linked processes. To this end, mitochondria were purified from HEK293 cells and resuspended in a medium that maintains mitochondria competent for import and translation (Figure 6B). Interestingly, we observed that under these translation-enabling conditions, the OXA1L protein was partially cleaved into four proteolytic fragments in TMEM126A<sup>-/-</sup> mitochondria, which could be detected with antibodies against C- and N-terminal epitopes (Figure 6C).

To define the proteases that facilitate OXA1L turnover in the inner membrane in the absence of TMEM126A, we depleted AFG3L2, PARL, SLP2, and YME1L, constituents of the *m*- and *i*AAA protease complexes, respectively.<sup>33,34</sup> Loss of the *i*AAA protease complex constituents PARL, SLP2, and YME1L, but not the loss of AFG3L2, blocked the observed OXA1L cleavage (Figure 6D).

We hypothesized that the observed reduced levels of mitochondrial translation products in the absence of TMEM126A were the result of increased turnover together with OXA1L. To test this, a simultaneous depletion of TMEM126A and YME1L was carried out. Indeed, although mitochondrial translation products were reduced upon TMEM126A depletion by 30%, translation products were fully recovered to WT levels upon additional depletion of YME1L (Figure 6E). We concluded that the observed partial OXA1L turnover upon loss of TMEM126A is coupled to mitochondrial quality control and that cargo-blocked complexes caused by the absence of TMEM126A are accessed and degraded by the mitochondrial *i*AAA protease.

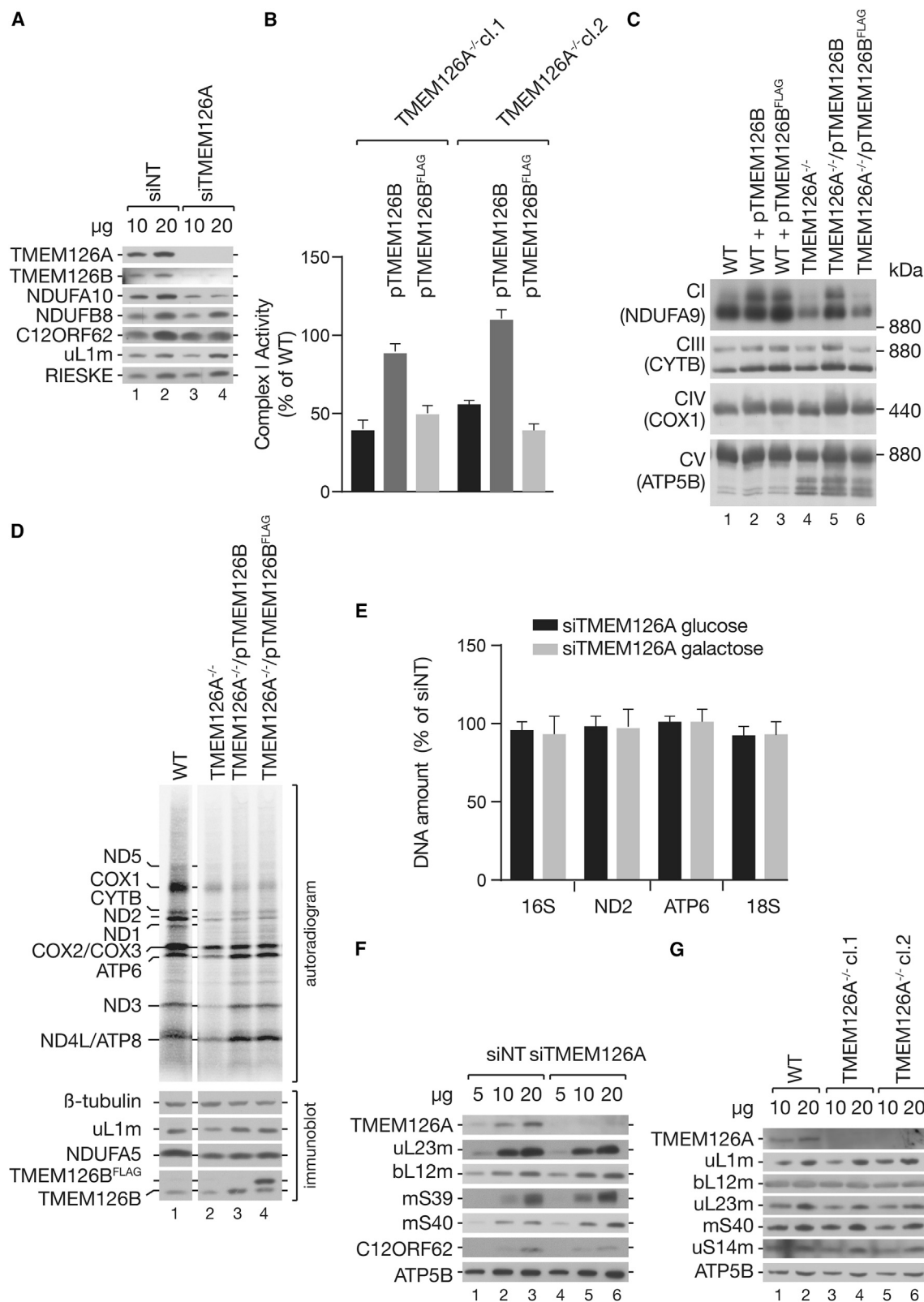
#### DISCUSSION

OXA1L facilitates the membrane insertion of mitochondrial- and selected nuclear-encoded proteins into the inner membrane. Several OXA1-related proteins with a similar membrane topology and transport function have been reported. Among these homologs are the chloroplast Alb3<sup>7,8,35,36</sup> and the bacterial YidC.<sup>9,10,37–39</sup> Based on structural and functional similarities, recent studies extended the group of OXA-related proteins to form the so-called OXA1 super-family, which includes subunits of ER protein translocation systems such as EMC3, TMCO1, and GET1.<sup>9</sup> Interestingly, EMC3 can functionally replace the mitochondrial yeast Oxa1 protein, demonstrating, in addition to similarities at the structural level, that these proteins are functionally conserved across bacteria, yeast, and human for membrane insertion.<sup>8</sup>

The OXA1L insertase machinery is functionally supplemented by accessory factors. In human mitochondria, translation

#### Figure 4. TMEM126A is required for complex I stability

(A) HEK293 cells were transfected with siRNA targeting TMEM126A or non-targeting (siNT) control. Cells were cultured in glucose media prior to harvesting and cell counting (SEM; n = 3) (left panel). Clones 1 and 2 of the TMEM126A<sup>-/-</sup> cells were seeded in glucose (middle panel) or galactose (right panel) containing media, cultured for 72 h and cells counted (SEM; n = 3). (B and C) Western blot analysis of mitochondrial proteins under loss of TMEM126A. Mitochondria from siTMEM126A treated cells (B) or TMEM126A<sup>-/-</sup> cells (C) were isolated and analyzed by western blotting using the indicated antibodies. (D and E) Mitochondria from siRNA-mediated TMEM126A depleted cells or TMEM126A<sup>-/-</sup> cells were solubilized in dodecylmaltoside (DDM). Cell lysates were subjected to BN-PAGE analysis (2.5%–10% gradient gel: CI, 4%–13% gradient gel: CII–CV), followed by western blotting using the indicated antibodies. See also Figure S3 and Table S3.



(legend on next page)

product-specific biogenesis factors, such as C12ORF62, SURF1, TMEM126B, TMEM177, or COX20, have been described to form complexes with OXA1L.<sup>22,28,29,40–43</sup> However, accessory interactors of OXA1L that function in a general manner on multiple or all translation products have not been described. Here, we identified TMEM126A as a protein associated with the OXA1L insertase in human mitochondria. About 70% of TMEM126A appear to form a complex with OXA1L when the endogenous proteins are analyzed. Both proteins bind to mitochondrial ribosomes and translation products. Our data are in agreement with the idea that OXA1L, together with TMEM126A, facilitates insertion of newly synthesized mitochondrial proteins into the inner membrane. Upon siRNA-mediated depletion and in TMEM126A knockout cells, a reduction of mitochondrial translation products was apparent. Interestingly, the amount of OXPHOS complexes, except for complex I, did not change substantially compared with the WT situation, although cell viability was affected. Hence, we speculate that the remaining protein synthesis, increased stability of translation products, or substituting factors suffice to maintain OXPHOS complexes. Recent work on the insertion of multispanning membrane proteins into the ER membrane revealed that this class of proteins requires specific chaperone-like factors to protect nascent transmembrane domains. The PAT and TMCO1 complexes of the ER fulfill such chaperone-like functions to cooperate with the Sec and EMC transport machineries for membrane insertion of multispanning proteins.<sup>9,44–46</sup> Corresponding proteins or complexes have not been described for the mitochondrial inner membrane despite the fact that mostly multispanning proteins are inserted by the OXA1L insertase. To this end, TMEM126A represents a likely candidate to act as a chaperone that works in concert with OXA1L.

Clogged translocases in the ER or the mitochondrial TOM complex can be accessed by a cytosolic quality control mechanism that removes precursor proteins and target these to the proteasome after ubiquitination.<sup>47–49</sup> However, the inner membrane of mitochondria is physically not accessible to these systems. Hence, alternative quality control pathways must be present to enable clearance of inner membrane translocases from miss-integrated proteins. It has been suggested that under stress conditions, a proteotoxicity arises within mitochondria, which triggers mitochondrial quality control and results in the degradation of mitochondrial-encoded nascent chains that fail to insert into the membrane.<sup>50,51</sup> Our data show that a lack of TMEM126A and the concomitant defect in mitochondrial protein biogenesis triggers a partial

turnover of the OXA1L insertase. The turnover of OXA1L appears to be predominantly mediated by the mitochondrial iAAA protease. Considering the reduced newly synthesized mitochondrial translation products upon loss of TMEM126A and the partial cleavage of OXA1L suggested that both processes are coupled. Indeed, depletion of YME1L suppresses OXA1L cleavage and recovers mitochondrial translation products in the absence of TMEM126A. We conclude that in agreement with the fact that OXA1L inserts proteins cotranslationally, its turnover occurs under cargo-stalled conditions. Accordingly, in the absence of a ubiquitin-proteasome system, which can remove precursor proteins from jammed translocases exposed to the cytosol, the mitochondrial inner membrane translocase is degraded. This situation is reminiscent of a report by van Stelten et al.<sup>52</sup> who demonstrated that in *E. coli* cells, in which the SEC translocon is jammed with a protein unable to pass the translocon, SecY, and its cargo are degraded by the AAA-protease FtsH, which is related to mitochondrial YME1L. Interestingly, the prohibitins Phb1 and Phb2 interact with Oxa1 in yeast. Loss of the prohibitins increases the turnover of Oxa1 by the YME1L.<sup>53</sup> Here, human PHB1 and PHB2 were also identified in mass spectrometric analysis of OXA1L. Hence, one could speculate that in the presence of TMEM126A, OXA1L stability is linked to prohibitins in the inner membrane preventing non-controlled degradation. In summary, we show that translocase jamming during transport of mitochondrial-encoded proteins activates quality control mechanisms at the inner membrane, which degrade the OXA1L insertase and newly made mitochondrial polypeptides. This process is apparent in the absence of the OXA1L-associated TMEM126A.

### Limitations of the study

Our study reveals the role of TMEM126A in protein transport into the inner mitochondrial membrane via the OXA1L insertase. However, studies in yeast mitochondria have also implicated the Oxa1 protein in membrane translocation of selected nuclear-encoded proteins or protein segments after their initial translocation into the matrix. It remains to be addressed if TMEM126A also contributes to this process or if its function is exclusively dedicated to those proteins that are inserted into the membrane co-translationally. A second open question of our study regards the relatively mild effect of a loss of TMEM126A on the steady-state level of the OXPHOS. It is tempting to speculate that mitochondria can partially adapt to loss of TMEM126A and that other proteins might be able to

### Figure 5. Reduction of TMEM126B levels affects complex I

(A) HEK293 cells were transfected with siRNA against TMEM126A, mitochondria isolated, and subjected to western blotting using indicated antibodies. (B and C) TMEM126A<sup>-/-</sup> cells were transfected with plasmids expressing TMEM126B or TMEM126B<sup>FLAG</sup> and activity of complex I measured (SEM, n = 3) (B). Alternatively, mitochondria were isolated, solubilized in dodecylmaltoside (DDM) and subjected to BN-PAGE analysis (C), followed by western blotting. (D) TMEM126B or TMEM126B<sup>FLAG</sup> were expressed in TMEM126A<sup>-/-</sup> as described in (B). Mitochondrial translation products were labeled with [<sup>35</sup>S]-methionine and proteins analyzed by SDS-PAGE and digital autoradiography. (E) HEK293 cells were transfected with siRNA targeting TMEM126A and cultured in glucose or galactose-containing media. mtDNA were isolated and mitochondrial DNA amounts quantified by qPCR (SEM, n = 3). (F and G) Mitochondria from HEK293 cells transfected with siTMEM126A (F) or TMEM126A<sup>-/-</sup> cells were isolated and subjected to western blot analysis using indicated antibodies. See also Figure S4.

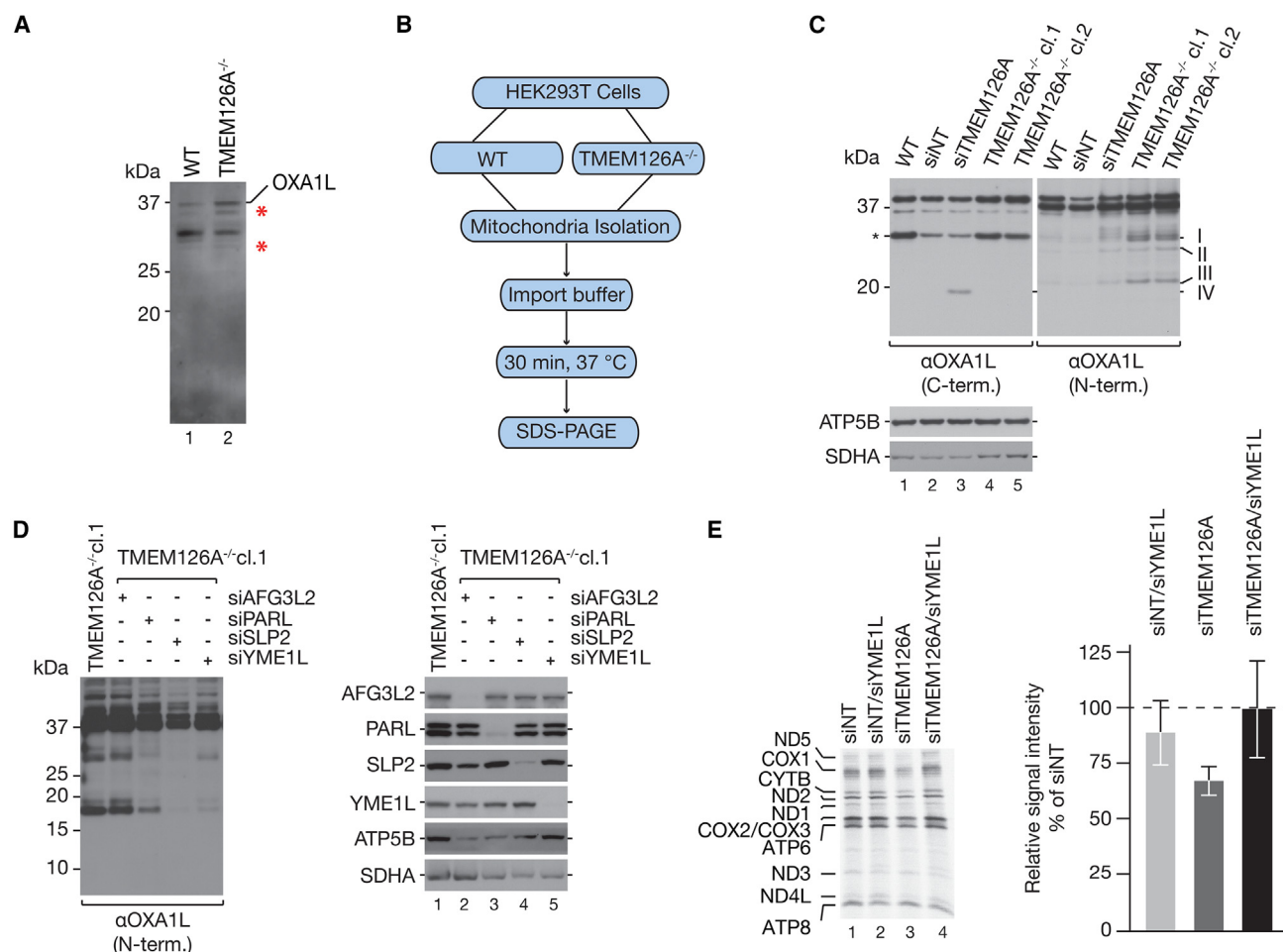


**Figure 6. Cargo insertion retardation activates mitochondrial quality control**

(A) OXA1L fragment analysis after whole-cell lysate of WT and TMEM126A<sup>-/-</sup> cells analyzed by western blot.  
 (B) Schematic presentation of experimental setup to monitor OXA1L fragmentation after quality control activation.  
 (C) Mitochondria isolated from siTMEM126A treated or TMEM126A<sup>-/-</sup> cells were analyzed as described in (B), subjected to western blotting using OXA1L antibodies.  
 (D) TMEM126A<sup>-/-</sup> cells were treated with siRNAs against AFG3L2, PARL, SLP2, and YME1L and isolated mitochondria treated as described in (A). Mitochondria were subsequently analyzed by western blotting and either OXA1L antibody applied to the whole membrane (left panel) or different antibodies (right panel) to confirm siRNA application and equal loading.  
 (E) Mitochondrial translation products were radiolabeled after siRNA-mediated depletion of TMEM126A or combined with siRNA against YME1L. HEK293 cell lysates were subjected to SDS-PAGE and analyses by digital autoradiography (left panel). Signals of three independent experiments were quantified (SEM; n = 3) (right panel).

compensate for this loss. Additional studies will be required to identify such proteins and their role in the process.

## STAR★METHODS

Detailed methods are provided in the online version of this paper and include the following:

### KEY RESOURCES TABLE

### RESOURCE AVAILABILITY

- Lead contact
- Materials availability
- Data and code availability

## EXPERIMENTAL MODEL AND STUDY PARTICIPANT DETAILS

- Cultivation of human cell lines

## METHOD DETAILS

- siRNA constructs and application
- [<sup>35</sup>S] methionine labelling of mitochondrial translation products
- NADH:ubiquinone reductase activity assay
- Quantification of mtDNA
- Isolation of mitochondria
- Protein localization and protease protection assays
- Affinity purification of protein complexes
- Cross-linking experiments

- Blue-Native-PAGE/ 2D-SDS-PAGE analysis
- Mass spectrometry
- **QUANTIFICATION AND STATISTICAL ANALYSIS**

## SUPPLEMENTAL INFORMATION

Supplemental information can be found online at <https://doi.org/10.1016/j.molcel.2023.12.013>.

## ACKNOWLEDGMENTS

We thank members of the Rehling laboratory for support and discussion. This study was funded by the Deutsche Forschungsgemeinschaft (DFG, German Research Foundation) under Germany's Excellence Strategy - EXC 2067/1-390729940 (P.R.) and CIBSS - EXC-2189 - project ID 390939984 (B.W.), SFB1190 (projects P13 [P.R.] and P23 [H.S.H.]), SFB1381 (project ID 403222702; B.W.), FOR2848 (projects P04 [P.R.] and P10 [H.S.H.], the European Research Council (ERC) Advanced Grant MiXpress (ERCAAdG no. 101095062) to P.R., DFG Emmy Noether grant (RI 2715/1-1 to R.R.-D.), and the Max Planck Society (P.R.).

## AUTHOR CONTRIBUTIONS

S.P., S.D., and P.R. developed the concept of the study. S.P., S.D., S.O., L.D.C.-Z., A.S., D.D., H.D., A.V., M.B., and J.S. performed the experiments. S.P., S.D., S.O., L.D.C.-Z., A.S., D.D., H.D., A.V., and L.S.K. analyzed the datasets and prepared the figures. S.D. and P.R. wrote the original draft. S.P., S.O., R.R.-D., H.S.H., B.W., S.D., and P.R. reviewed and edited the final draft of the manuscript. S.D. and P.R. provided supervision.

## DECLARATION OF INTERESTS

The authors declare no competing interests

Received: February 23, 2023

Revised: October 17, 2023

Accepted: December 8, 2023

Published: January 9, 2024

## REFERENCES

- Pearce, S.F., Rebelo-Guiomar, P., D'Souza, A.R., Powell, C.A., Van Haute, L., and Minczuk, M. (2017). Regulation of mammalian mitochondrial gene expression: recent advances. *Trends Biochem. Sci.* 42, 625–639.
- Hällberg, B.M., and Larsson, N.G. (2014). Making proteins in the powerhouse. *Cell Metab.* 20, 226–240.
- Pfanner, N., Warscheid, B., and Wiedemann, N. (2019). Mitochondrial proteins: from biogenesis to functional networks. *Nat. Rev. Mol. Cell Biol.* 20, 267–284.
- Dennerlein, S., Poerschke, S., Oeljeklaus, S., Wang, C., Richter-Dennerlein, R., Sattmann, J., Bauermeister, D., Hanitsch, E., Stoldt, S., Langer, T., et al. (2021). Defining the interactome of the human mitochondrial ribosome identifies SMIM4 and TMEM223 as respiratory chain assembly factors. *eLife* 10, e68213.
- Fernández-Vizarra, E., and Zeviani, M. (2021). Mitochondrial disorders of the OXPHOS system. *FEBS Lett.* 595, 1062–1106.
- Hock, D.H., Robinson, D.R.L., and Stroud, D.A. (2020). Blackout in the powerhouse: clinical phenotypes associated with defects in the assembly of OXPHOS complexes and the mitoribosome. *Biochem. J.* 477, 4085–4132.
- Funes, S., Kauff, F., van der Sluis, E.O., Ott, M., and Herrmann, J.M. (2011). Evolution of YidC/Oxa1/Alb3 insertases: three independent gene duplications followed by functional specialization in bacteria, mitochondria and chloroplasts. *Biol. Chem.* 392, 13–19.
- Güngör, B., Flohr, T., Garg, S.G., and Herrmann, J.M. (2022). The ER membrane complex (EMC) can functionally replace the Oxa1 insertase in mitochondria. *PLoS Biol.* 20, e3001380.
- Hegde, R.S., and Keenan, R.J. (2022). The mechanisms of integral membrane protein biogenesis. *Nat. Rev. Mol. Cell Biol.* 23, 107–124.
- Homborg, B., Rehling, P., and Cruz-Zaragoza, L.D. (2023). The multifaceted mitochondrial OXA insertase. *Trends Cell Biol.* 33, 765–772.
- Jia, L., Dienhart, M., Schrapf, M., McCauley, M., Hell, K., and Stuart, R.A. (2003). Yeast Oxa1 interacts with mitochondrial ribosomes: the importance of the C-terminal region of Oxa1. *EMBO J.* 22, 6438–6447.
- Haque, M.E., Elmore, K.B., Tripathy, A., Koc, H., Koc, E.C., and Spremulli, L.L. (2010). Properties of the C-terminal tail of human mitochondrial inner membrane protein Oxa1L and its interactions with mammalian mitochondrial ribosomes. *J. Biol. Chem.* 285, 28353–28362.
- Kohler, R., Boehringer, D., Greber, B., Bingel-Erlenmeyer, R., Collinson, I., Schaffitzel, C., and Ban, N. (2009). YidC and Oxa1 form dimeric insertion pores on the translating ribosome. *Mol. Cell* 34, 344–353.
- Szyrach, G., Ott, M., Bonnefoy, N., Neupert, W., and Herrmann, J.M. (2003). Ribosome binding to the Oxa1 complex facilitates co-translational protein insertion in mitochondria. *EMBO J.* 22, 6448–6457.
- He, S., and Fox, T.D. (1997). Membrane translocation of mitochondrially coded Cox2p: distinct requirements for export of N and C termini and dependence on the conserved protein Oxa1p. *Mol. Biol. Cell* 8, 1449–1460.
- Hell, K., Neupert, W., and Stuart, R.A. (2001). Oxa1p acts as a general membrane insertion machinery for proteins encoded by mitochondrial DNA. *EMBO J.* 20, 1281–1288.
- Stuart, R. (2002). Insertion of proteins into the inner membrane of mitochondria: the role of the Oxa1 complex. *Biochim. Biophys. Acta* 1592, 79–87.
- Bohnert, M., Rehling, P., Guiard, B., Herrmann, J.M., Pfanner, N., and van der Laan, M. (2010). Cooperation of stop-transfer and conservative sorting mechanisms in mitochondrial protein transport. *Curr. Biol.* 20, 1227–1232.
- Fiumera, H.L., Dunham, M.J., Saracco, S.A., Butler, C.A., Kelly, J.A., and Fox, T.D. (2009). Translocation and assembly of mitochondrially coded *Saccharomyces cerevisiae* cytochrome c oxidase subunit Cox2 by Oxa1 and Yme1 in the absence of Cox18. *Genetics* 182, 519–528.
- Stiller, S.B., Höpker, J., Oeljeklaus, S., Schütze, C., Schrempp, S.G., Vent-Schmidt, J., Horvath, S.E., Frazier, A.E., Gebert, N., van der Laan, M., et al. (2016). Mitochondrial OXA translocase plays a major role in biogenesis of inner-membrane proteins. *Cell Metab.* 23, 901–908.
- Stiburek, L., Fomuskova, D., Wenchich, L., Pejznochova, M., Hansikova, H., and Zeman, J. (2007). Knockdown of human Oxa1l impairs the biogenesis of F1Fo-ATP synthase and NADH:ubiquinone oxidoreductase. *J. Mol. Biol.* 374, 506–516.
- Thompson, K., Mai, N., Oláhová, M., Scialó, F., Formosa, L.E., Stroud, D.A., Garrett, M., Lax, N.Z., Robertson, F.M., Jou, C., et al. (2018). OXA1L mutations cause mitochondrial encephalopathy and a combined oxidative phosphorylation defect. *EMBO Mol. Med.* 10, e9060.
- Itoh, Y., Andréll, J., Choi, A., Richter, U., Maiti, P., Best, R.B., Barrientos, A., Battersby, B.J., and Amunts, A. (2021). Mechanism of membrane-tethered mitochondrial protein synthesis. *Science* 371, 846–849.
- Gomkale, R., Linden, A., Neumann, P., Schendzielorz, A.B., Stoldt, S., Dybkov, O., Kilisch, M., Schulz, C., Cruz-Zaragoza, L.D., Schwappach, B., et al. (2021). Mapping protein interactions in the active TOM-TIM23 supercomplex. *Nat. Commun.* 12, 5715.
- Richter, F., Dennerlein, S., Nikolov, M., Jans, D.C., Naumenko, N., Aich, A., MacVicar, T., Linden, A., Jakobs, S., Urlaub, H., et al. (2019). ROMO1 is a constituent of the human presequence translocase required for YME1L protease import. *J. Cell Biol.* 218, 598–614.



26. Frazier, A.E., Taylor, R.D., Mick, D.U., Warscheid, B., Stoepel, N., Meyer, H.E., Ryan, M.T., Guiard, B., and Rehling, P. (2006). Mdm38 interacts with ribosomes and is a component of the mitochondrial protein export machinery. *J. Cell Biol.* **172**, 553–564.
27. Hanein, S., Garcia, M., Fares-Taie, L., Serre, V., De Keyser, Y., Delaveau, T., Perrault, I., Delphin, N., Gerber, S., Schmitt, A., et al. (2013). TMEM126A is a mitochondrial located mRNA (MLR) protein of the mitochondrial inner membrane. *Biochim. Biophys. Acta* **1830**, 3719–3733.
28. Formosa, L.E., Reljić, B., Sharpe, A.J., Hock, D.H., Muellner-Wong, L., Stroud, D.A., and Ryan, M.T. (2021). Optic atrophy-associated TMEM126A is an assembly factor for the ND4-module of mitochondrial complex I. *Proc. Natl. Acad. Sci. USA* **118**, e2019665118.
29. D'Angelo, L., Astro, E., De Luise, M., Kurelac, I., Umesh-Ganesh, N., Ding, S., Fearnley, I.M., Gasparre, G., Zeviani, M., Porcelli, A.M., et al. (2021). NDUF53 depletion permits complex I maturation and reveals TMEM126A/OPA7 as an assembly factor binding the ND4-module intermediate. *Cell Rep.* **35**, 109002.
30. Rath, S., Sharma, R., Gupta, R., Ast, T., Chan, C., Durham, T.J., Goodman, R.P., Grabarek, Z., Haas, M.E., Hung, W.H.W., et al. (2021). MitoCarta3.0: an updated mitochondrial proteome now with sub-organelle localization and pathway annotations. *Nucleic Acids Res.* **49**, D1541–D1547.
31. Hell, K., Herrmann, J.M., Pratje, E., Neupert, W., and Stuart, R.A. (1998). Oxa1p, an essential component of the N-tail protein export machinery in mitochondria. *Proc. Natl. Acad. Sci. USA* **95**, 2250–2255.
32. Wang, C., Richter-Dennerlein, R., Pacheu-Grau, D., Liu, F., Zhu, Y., Dennerlein, S., and Rehling, P. (2020). MITRAC15/COA1 promotes mitochondrial translation in a ND2 ribosome-nascent chain complex. *EMBO Rep.* **21**, e48833.
33. Quirós, P.M., Langer, T., and López-Otín, C. (2015). New roles for mitochondrial proteases in health, ageing and disease. *Nat. Rev. Mol. Cell Biol.* **16**, 345–359.
34. Deshwal, S., Fiedler, K.U., and Langer, T. (2020). Mitochondrial proteases: multifaceted regulators of mitochondrial plasticity. *Annu. Rev. Biochem.* **89**, 501–528.
35. Jiang, F., Yi, L., Moore, M., Chen, M., Rohl, T., Van Wijk, K.J., De Gier, J.W., Henry, R., and Dalbey, R.E. (2002). Chloroplast YidC homolog Albino3 can functionally complement the bacterial YidC depletion strain and promote membrane insertion of both bacterial and chloroplast thylakoid proteins. *J. Biol. Chem.* **277**, 19281–19288.
36. Moore, M., Goforth, R.L., Mori, H., and Henry, R. (2003). Functional interaction of chloroplast SRP/FtsY with the ALB3 translocase in thylakoids: substrate not required. *J. Cell Biol.* **162**, 1245–1254.
37. Preuss, M., Ott, M., Funes, S., Lührink, J., and Herrmann, J.M. (2005). Evolution of mitochondrial oxa proteins from bacterial YidC. Inherited and acquired functions of a conserved protein insertion machinery. *J. Biol. Chem.* **280**, 13004–13011.
38. van Bloois, E., Nagamori, S., Koningsstein, G., Ullers, R.S., Preuss, M., Oudega, B., Harms, N., Kaback, H.R., Herrmann, J.M., and Lührink, J. (2005). The Sec-independent function of *Escherichia coli* YidC is evolutionary-conserved and essential. *J. Biol. Chem.* **280**, 12996–13003.
39. Samuelson, J.C., Chen, M., Jiang, F., Möller, I., Wiedmann, M., Kuhn, A., Phillips, G.J., and Dalbey, R.E. (2000). YidC mediates membrane protein insertion in bacteria. *Nature* **406**, 637–641.
40. Richter-Dennerlein, R., Oeljeklaus, S., Lorenzi, I., Ronsör, C., Bareth, B., Schendzielorz, A.B., Wang, C., Warscheid, B., Rehling, P., and Dennerlein, S. (2016). Mitochondrial protein synthesis adapts to influx of nuclear-encoded protein. *Cell* **167**, 471–483.e10.
41. Bourens, M., Boulet, A., Leary, S.C., and Barrientos, A. (2014). Human COX20 cooperates with SCO1 and SCO2 to mature COX2 and promote the assembly of cytochrome c oxidase. *Hum. Mol. Genet.* **23**, 2901–2913.
42. Lorenzi, I., Oeljeklaus, S., Aich, A., Ronsör, C., Callegari, S., Dudek, J., Warscheid, B., Dennerlein, S., and Rehling, P. (2018). The mitochondrial TMEM177 associates with COX20 during COX2 biogenesis. *Biochim. Biophys. Acta Mol. Cell Res.* **1865**, 323–333.
43. Agostino, A., Invernizzi, F., Tiveron, C., Fagioli, G., Prella, A., Lamantea, E., Giavazzi, A., Battaglia, G., Tatangelo, L., Tiranti, V., et al. (2003). Constitutive knockout of Surf1 is associated with high embryonic lethality, mitochondrial disease and cytochrome c oxidase deficiency in mice. *Hum. Mol. Genet.* **12**, 399–413.
44. Chitwood, P.J., and Hegde, R.S. (2020). An intramembrane chaperone complex facilitates membrane protein biogenesis. *Nature* **584**, 630–634.
45. Smalinskaitė, L., Kim, M.K., Lewis, A.J.O., Keenan, R.J., and Hegde, R.S. (2022). Mechanism of an intramembrane chaperone for multipass membrane proteins. *Nature* **611**, 161–166.
46. Sundaram, A., Yamsek, M., Zhong, F., Hooda, Y., Hegde, R.S., and Keenan, R.J. (2022). Substrate-driven assembly of a translocon for multipass membrane proteins. *Nature* **611**, 167–172.
47. Song, J., and Becker, T. (2022). Fidelity of organellar protein targeting. *Curr. Opin. Cell Biol.* **75**, 102071.
48. Schulte, U., Brave, den, F., Haupt, A., Gupta, A., Song, J., Müller, C.S., Engelke, J., Mishra, S., Mårtensson, C., Ellenrieder, L., et al. (2023). Mitochondrial complexome reveals quality-control pathways of protein import. *Nature* **614**, 153–159.
49. Bragoszewski, P., Wasilewski, M., Sakowska, P., Gornicka, A., Böttinger, L., Qiu, J., Wiedemann, N., and Chacinska, A. (2015). Retro-translocation of mitochondrial intermembrane space proteins. *Proc. Natl. Acad. Sci. USA* **112**, 7713–7718.
50. Richter, U., Lahtinen, T., Martinen, P., Suomi, F., and Battersby, B.J. (2015). Quality control of mitochondrial protein synthesis is required for membrane integrity and cell fitness. *J. Cell Biol.* **211**, 373–389.
51. Richter, U., Ng, K.Y., Suomi, F., Martinen, P., Turunen, T., Jackson, C., Suomalainen, A., Vihinen, H., Jokitalo, E., Nyman, T.A., et al. (2019). Mitochondrial stress response triggered by defects in protein synthesis quality control. *Life Sci. Alliance* **2**, e201800219.
52. van Stelten, J., Silva, F., Belin, D., and Silhavy, T.J. (2009). Effects of antibiotics and a proto-oncogene homolog on destruction of protein translocator SecY. *Science* **325**, 753–756.
53. Käser, M., and Langer, T. (2000). Protein degradation in mitochondria. *Semin. Cell Dev. Biol.* **11**, 181–190.
54. Mick, D.U., Dennerlein, S., Wiese, H., Reinhold, R., Pacheu-Grau, D., Lorenzi, I., Sasarman, F., Weraarpachai, W., Shoubridge, E.A., Warscheid, B., et al. (2012). MITRAC links mitochondrial protein translocation to respiratory-chain assembly and translational regulation. *Cell* **151**, 1528–1541.
55. Ran, F.A., Hsu, P.D., Lin, C.Y., Gootenberg, J.S., Konermann, S., Trevino, A.E., Scott, D.A., Inoue, A., Matoba, S., Zhang, Y., et al. (2013). Double nicking by RNA-guided CRISPR Cas9 for enhanced genome editing specificity. *Cell* **154**, 1380–1389.
56. Vakulskas, C.A., C.A., Dever, D.P., Rettig, G.R., Turk, R., Jacobi, A.M., Collingwood, M.A., Bode, N.M., McNeill, M.S., Yan, S., Camarena, J., et al. (2018). A high-fidelity Cas9 mutant delivered as a ribonucleoprotein complex enables efficient gene editing in human hematopoietic stem and progenitor cells. *Nat. Med.* **24**, 1216–1224.
57. Panov, A., and Orynbayeva, Z. (2013). Bioenergetic and antiapoptotic properties of mitochondria from cultured human prostate cancer cell lines PC-3, DU145 and LNCaP. *PLoS One* **8**, e72078.
58. Cruz-Zaragoza, L.D., Dennerlein, S., Linden, A., Yousefi, R., Lavdovskaia, E., Aich, A., Falk, R.R., Gorkale, R., Schöndorf, T., Bohnsack, M.T., et al. (2021). An *in vitro* system to silence mitochondrial gene expression. *Cell* **184**, 5824–5837.e15.
59. Wittig, I., Braun, H.P., and Schägger, H. (2006). Blue native PAGE. *Nat. Protoc.* **1**, 418–428.

60. Cox, J., and Mann, M. (2008). MaxQuant enables high peptide identification rates, individualized p.p.b.-range mass accuracies and proteome-wide protein quantification. *Nat. Biotechnol.* **26**, 1367–1372.
61. Cox, J., Neuhauser, N., Michalski, A., Scheltema, R.A., Olsen, J.V., and Mann, M. (2011). Andromeda: a peptide search engine integrated into the MaxQuant environment. *J. Proteome Res.* **10**, 1794–1805.
62. Bolstad, B.M., Irizarry, R.A., Astrand, M., and Speed, T.P. (2003). A comparison of normalization methods for high density oligonucleotide array data based on variance and bias. *Bioinformatics* **19**, 185–193.
63. Verboven, S., Branden, K.V., and Goos, P. (2007). Sequential imputation for missing values. *Comput. Biol. Chem.* **31**, 320–327.

# STAR★METHODS

## KEY RESOURCES TABLE

REAGENT or RESOURCE	SOURCE	IDENTIFIER
<b>Antibodies</b>		
Rabbit polyclonal anti-AFG3L2	This paper	#4826
Rabbit polyclonal anti-ATP5B	This paper	#4826
Rabbit polyclonal anti-COX1	This paper	#5120
Rabbit polyclonal anti-COX2	Abcam	Cat# AB110258; RRID: AB_10887758
Rabbit polyclonal anti-COX4-I	This paper	#1522
Rabbit polyclonal anti-COX5B	This paper	#4965
Rabbit polyclonal anti-COX6A	This paper	#3282
Rabbit polyclonal anti-C12ORF62	This paper	#4844
Rabbit polyclonal anti-C12ORF73	This paper	#5104
Rabbit polyclonal anti-CYTB	This paper	#5151
Rabbit polyclonal anti-GTPBP10	Novus Bio	Cat#NBP1-85055; RRID: AB_11037644
Rabbit polyclonal anti-MITRAC12	This paper	#3761
Rabbit polyclonal anti-NDUFA5	Proteintech	Cat#16640-1-AP; RRID: AB_2251270
Rabbit polyclonal anti-NDUFA9	This paper	#1524
Rabbit polyclonal anti-NDUFAF4	Proteintech	Cat#26003-1-AP; RRID: AB_2880329
Rabbit polyclonal anti-NDUFB8	This paper	#3764
Rabbit polyclonal anti-NDUFB10	Proteintech	Cat#15589-1-AP; RRID: AB_2150790
Rabbit polyclonal anti-NDUFB11	Proteintech	Cat# 16720-1-AP; RRID: AB_2298378
Rabbit polyclonal anti-NDUFS1	Proteintech	Cat#12444-1-AP; RRID: AB_2282657
Rabbit polyclonal anti-OCIAD2	This paaper	NA
Rabbit polyclonal anti-OXA1L N-terminal	This paaper	#5095
Rabbit polyclonal anti-OXA1L C-terminal	This paaper	#5035
Rabbit polyclonal anti-PARL	Proteintech	Cat#26679-1-AP; RRID: AB_2880599
Rabbit polyclonal anti-PHB2	Proteintech	Cat#12295-1-AP; RRID: AB_2164779
Rabbit polyclonal anti-RIESKE	This paper	#1512
Mouse monoclonal anti-SDHA	ThermoFisher Scientific	Cat# 459200; RRID: AB_2532231
Rabbit polyclonal anti-TACO1	This paper	#3628
Rabbit polyclonal anti-TIM23	This paper	#1526
Rabbit polyclonal anti-TIM21	This paper	#3674
Rabbit polyclonal anti-TOM20	Proteintech	Cat# 11802-1-AP; RRID: AB_2207530
Rabbit polyclonal anti-uL1m	This paper	#4964
Rabbit polyclonal anti-bL12m	Proteintech	Cat# 14795-1-AP; RRID: AB_2250805
Rabbit polyclonal anti-uL23m	This paper	#1716
Rabbit polyclonal anti-mL45	Proteintech	Cat# 15682-1-AP; RRID: AB_2146065
Rabbit polyclonal anti-mL62	This paper	#5131
Rabbit polyclonal anti-uS17m	Proteintech	Cat#18881-1-AP; RRID: AB_10597844
Rabbit polyclonal anti-uS14m	Proteintech	Cat# 16301-1-AP; RRID: AB_2878240
Rabbit polyclonal anti-uS15m	Proteintech	Cat# 17006-1-AP; RRID: AB_2301068
Rabbit polyclonal anti-mS39	Sigma Prestige	Cat#HPA041154; RRID: AB_10795488
Rabbit polyclonal anti-mS40	This paper	#5177
Rabbit polyclonal anti-SLP2	Proteintech	Cat# 10348-1-AP; RRID: AB_2286822
Rabbit polyclonal anti-TMEM126A	This paper	#5170
Rabbit polyclonal anti-TMEM126B	This paper	#5250

(Continued on next page)

**Continued**

REAGENT or RESOURCE	SOURCE	IDENTIFIER
Rabbit polyclonal anti-TMEM177	This paper	#4988
Rabbit polyclonal anti-UQCC2	This paper	#5253
Rabbit polyclonal anti-VDAC	This paper	#1515
Rabbit polyclonal anti-YME1L	Proteintech	#11510-1-AP; RRID: AB_2217459
Goat anti-Rabbit IgG (H+L) HRPO	Jackson ImmunoResearch	Cat# 111-035-144, RRID:AB_2307391
Goat anti-Mouse IgG (H+L) HRPO	Jackson ImmunoResearch	Cat# 115-035-166 RRID: AB_2338511

**Chemicals, peptides, and recombinant proteins**

Digitonin	Merck Millipore	Cat# 300410
anti-FLAG M2 Affinity Gel	Sigma-Aldrich	Cat# A2220
[ <sup>35</sup> S] methionine	Hartmann Analytic	Cat# SCM-01
Lipofectamine RNAiMAX	Invitrogen	Cat# 13778075
GeneJuice™	Sigma-Aldrich	Cat# 70967

**Critical commercial assays**

nCounter® XT TagSet24	nanoString	N/A
KOD Hot Start DNA Polymerase	Merck	Cat# 71086-3
TaqMan™ Schneller Advanced Master-Mix	Applied Biosystems™	4444556
Complex I Enzyme Activity Microplate Kit	Abcam	ab109721

**Deposited data**

Raw data	This study	<a href="https://data.mendeley.com/v1/datasets/publish-confirmation/hhf6hmcrrw/1?folder=">https://data.mendeley.com/v1/datasets/publish-confirmation/hhf6hmcrrw/1?folder=</a>
----------	------------	---

**Experimental models: Cell lines**

HEK293-Flp-In™ T-Rex™ (HEK293T)	ThermoFisher Scientific	RRID: CVCL_U421
HEK293T- <sup>FLAG</sup> OXA1L (aa74)	This paper	N/A
HEK293T-OXA1L <sup>FLAG</sup> (aa326)	This paper	N/A
HEK293T-OXA1L <sup>FLAG</sup> (aa397)	This paper	N/A

**Oligonucleotides**

AFG3L2 siRNA: GCUCUUGGAUA GGAUGUGU	Eurogentec	N/A
OXA1L siRNA: ACCACUGGCAGU CACUGCUACAAU	Eurogentec	N/A
PARL siRNA CCAGCGGACUGUG ACAGGUUUUAUA	Eurogentec	N/A
SLP2 siRNA: GCAUUGUGGAUG CCAUCAA	Eurogentec	N/A
TMEM126A siRNA: GGUGAUUUG GAUUGUGAAA	Eurogentec	N/A
YME1L siRNA: UUCGAUGGCAGA UUGGGUUUCUGGA	Eurogentec	N/A
MT-RNR2	Applied Biosystems™	Hs02596860_s1
MT-ND2	Applied Biosystems™	Hs02596874_g1
18s rRNA	Applied Biosystems™	Hs99999901_s1
MT-ATP6	Applied Biosystems™	Hs02596862_g1

**Recombinant DNA**

pcDNA3.1_TMEM126B	This study/ Genscript	N/A
pcDNA3.1_TMEM126B <sup>FLAG</sup>	This study	N/A

(Continued on next page)

### Continued

REAGENT or RESOURCE	SOURCE	IDENTIFIER
pcDNA5-FLAG-OXA1L (aa74)	This study	N/A
pcDNA5-OXA1L <sup>FLAG</sup> (aa326)	This study	N/A
pcDNA5-OXA1L <sup>FLAG</sup> (aa397)	This study	N/A
<b>Software and algorithms</b>		
ImageQuantTL v8.1	GE Healthcare	<a href="https://www.gelifesciences.com/en/us/shop/protein-analysis/molecular-imaging-for-proteins/imaging-software/imagequant-tl-8-1-p-00110">https://www.gelifesciences.com/en/us/shop/protein-analysis/molecular-imaging-for-proteins/imaging-software/imagequant-tl-8-1-p-00110</a>
ImageJ v1.47	NIH	<a href="https://imagej.nih.gov/ij/download.html">https://imagej.nih.gov/ij/download.html</a>
Prism 8	GraphPad Software	<a href="https://www.graphpad.com/scientific-software/prism/">https://www.graphpad.com/scientific-software/prism/</a>
nSolver	nanoString	<a href="https://www.nanostring.com/products/analysis-solutions/ncounter-analysis-solutions/">https://www.nanostring.com/products/analysis-solutions/ncounter-analysis-solutions/</a>

## RESOURCE AVAILABILITY

### Lead contact

Further information and requests for resources and reagents should be directed to and will be fulfilled by the lead contact, Peter Rehling ([peter.rehling@medizin.uni-goettingen.de](mailto:peter.rehling@medizin.uni-goettingen.de)).

### Materials availability

This study did not generate new unique reagents.

### Data and code availability

- All data from the mass spectrometry analyses are provided as Supplemented Excel file Tables within the manuscript.
- This paper does not report original code.
- Any additional information required to reanalyze the data reported in this paper is available from the [lead contact](#) upon request.

Mendeley Data can be found: <https://data.mendeley.com/v1/datasets/publish-confirmation/hhf6hmcrrw/1?folder=>

## EXPERIMENTAL MODEL AND STUDY PARTICIPANT DETAILS

### Cultivation of human cell lines

Human embryonic kidney cell lines (HEK293; Thermo Fisher Scientific) were cultured in a humidified atmosphere at 37°C, 5% CO<sub>2</sub> in standard Dulbecco's modified Eagle's medium (DMEM), containing either glucose (4.5 mg/ml) or galactose (0.9 mg/ml), which was supplemented with 10% (v/v) fetal bovine serum (FBS, Capricorn Scientific), 1 mM sodium pyruvate, 2 mM L-glutamine and 50 µg/ml uridine. Cell counts were performed with a Neubauer counting chamber. All cultured cell lines were checked for mycoplasma on a regular basis (Eurofins Genomics). The under control of a tetracycline inducible CMC promotor expressing cell line <sup>FLAG</sup>OXA1L (NM\_005015.3) was generated as described previously.<sup>54</sup> The TMEM126A<sup>-/-</sup> cell line was produced by transfecting the guide RNA (AGTCAGTCCACTCCGTGTATGG), which was fused to a tracer RNA in a complex with the CAS9 enzyme as described previously.<sup>55,56</sup> Single cells were sorted by flow cytometry 24 h after transfection. Single colonies were screened by immunoblotting and sequencing of the corresponding gene region. For SILAC analysis, cells were cultured as previously described.<sup>54</sup> To inhibit mitochondrial translation, Thiamphenicol (50 µg/ml final) was added to the tissue culture media. Within the analysis of the OXA1L fragments we discovered that different patches of FCS (fetal calve serum) could lead to different outcome of experiments. Therefore, for analysis of OXA1L-fragments, we cultured the cells for 24h in FCS free media. Isolated mitochondria were incubated in sucrose buffer (250 mM sucrose, pH 7.4; 80 mM K-acetate, 5 mM Mg-acetate, 10 mM sodium succinate, 20 mM HEPES) for 30 min at 37°C.



## METHOD DETAILS

### siRNA constructs and application

For siRNA mediated reduction of AFG3L2 (GCUCUUGGAUAGGAUGUGU), OXA1L (ACC-ACU-GGC-AGU-CAC-UGC-UAC-AAU), PARL (CCAGCGGACUGUGACAGGUAUUUAUA), SLP2 (GCAUUGUGGAUGCCAUCAA), TMEM126A (GGU-GAU-UUG-GAU-UGU-GAA-A), OXA1L (ACC-ACU-GGC-AGU-CAC-UGC-UAC-AAU) transient transfection of siRNA oligonucleotides and control siRNA molecules (each final 33 nM) into HEK293 WT cells was performed. To do so, Lipofectamine RNAi-MAX (Invitrogen) was used, following the manufacturer's protocol. In general, cells were incubated under standard tissue culture conditions for 72 h.

### [<sup>35</sup>S] methionine labelling of mitochondrial translation products

To incorporate [<sup>35</sup>S] methionine into newly synthesized mitochondrial proteins, first cells were starved with FCS/methionine-free media. Cytosolic translation was either inhibited with emetine dihydrochloride hydrate (final 100 µg/ml, Sigma-Aldrich) for pulse experiments or with anisomycin (final 100 µg/ml, Sigma-Aldrich) for pulse-chase experiments. Cells were incubated for defined time points with 0.2 mCi/ml [<sup>35</sup>S] methionine in standard DMEM without methionine. For further analysis, cells were harvested and washed with PBS. Radioactive signals were detected by autoradiography, using Storage Phosphor Screens via a Typhoon FLA 7000 scanner (GE Healthcare).

### NADH:ubiquinone reductase activity assay

To determine the complex I enzyme activity a microplate assay kit was used according to the manufacturer's protocol (ab109721, abcam). 20 µg of isolated mitochondria or cell lysates were used for each measurement at 450 nm as described previously.<sup>32</sup> The complex I activity was calculated using the linear rate of increase in absorbance over time.

### Quantification of mtDNA

genomic DNA was isolated with the Purelink Genomic DNA kit (Invitrogen, K1820-01) following the manufacturer's protocol. Briefly, cells were harvested with PBS and 20 µl of Proteinase K and 20 µl RNase A added. After 2 min incubation, 200 µl of lysis buffer were added, the samples 10 min incubated at 55°C, followed by EtOH addition (200 µl). The DNA was bound as described in the kit and eluted in 100 µl elution buffer. qPCR was performed using the TaqMan Universal PCR Master Mix (Thermo Fisher Scientific, 1901150). As TaqMan probes were purchased from Thermo Fisher Scientific (ATP6:Hs02596862\_g1, ND2 Hs02596874\_g1, MT-RNR2 Hs02596860\_s1, 18S Hs99999901\_s1). The amplification program was followed as suggested by the manufacturer.

### Isolation of mitochondria

For mitochondria isolation, the protocol of Panov and Orynbayeva,<sup>57</sup> slightly modified, was followed. First, cells were harvested with PBS and for homogenization resuspended in cold TH-buffer, containing 300 mM Trehalose, 10 mM KCl, 10 mM HEPES (pH 7.4), 2 mM PMSF and 0.1 mg BSA/ml. Cells were opened gently by two times homogenization (30 strokes each) using a dounce homogenizer (800 rpm/min). For the "fast" mitochondrial isolation (Figure S4A), cells were homogenized only once (40 strokes). Unbroken cells were pelleted 'time at 400 x g for 10 min at 4°C. Left over cells were removed by centrifugation (800 x g, 8 min, 4°C) and the mitochondria containing supernatant collected. Afterward, mitochondria were collected at 11,000 x g, 10 min, 4°C, pooled and washed with BSA-free TH-buffer. Mitochondria concentration was determined by Bradford and mitochondria were used immediately or stored at -80°C. For analysis of OXA1L-fragments, isolated mitochondria were incubated in sucrose buffer (250 mM sucrose, pH 7.4; 80 mM K-acetate, 5 mM Mg-acetate, 10 mM sodium succinate, 20 mM HEPES) for 30 min at 37°C.

### Protein localization and protease protection assays

To investigate the submitochondrial localization of proteins, fresh isolated mitochondria were either resuspended in osmotic stabilizing SEM buffer (250 mM sucrose, 1 mM EDTA, and 10 mM MOPS [pH 7.2]), or, to rupture the outer mitochondrial membrane, in non-osmotic EM buffer (1 mM EDTA, 10 mM MOPS [pH 7.2]). Subsequently, samples were treated with Proteinase K (PK) for 10 min on ice. Mitochondria were lysed by sonication in the presence of PK. To inactivate PK, samples were PMSF treated at a final concentration of 2 mM and incubated on ice for 10 min. Finally, samples were supplemented with 2 x SDS loading buffer and incubated for 5 min at 95 °C.

### Affinity purification of protein complexes

Isolated mitochondria or cells were lysed in solubilization buffer (150 mM NaCl, 10% glycerol (v/v), 20 mM MgCl<sub>2</sub>, 2 mM PMSF, 50 mM Tris-HCl, pH 7.4, 1% digitonin (v/w), protease inhibitor) in a ratio of 1–2 µg/µl for 30 min at 4 °C with gentle agitation. Lysates were cleared by centrifugation (15 min, 16,000 x g, 4°C) and transferred onto anti-FLAG M2 agarose beads (Sigma-Aldrich) for FLAG immunoprecipitation. After 1 h binding at 4°C, beads were washed ten times with washing buffer (50 mM Tris-HCl, pH 7.4, 150 mM NaCl, 10% glycerol (v/v), 20 mM MgCl<sub>2</sub>, 1 mM PMSF, 0.3% digitonin (v/w)) to remove unbound proteins. Bound proteins were eluted with FLAG peptide (Sigma-Aldrich) for 30 min at 4°C, gentle agitating. Samples were analyzed by SDS-PAGE and immunoblotting or quantitative mass spectrometry. For antibody immunoprecipitation, the same protocol was used as described above. Lysed mitochondria or cells were transferred onto protein A-Sepharose (PAS) containing crosslinked TMEM126A or OXA1L antibody in a

Mobicol spin column (MoBiTec). Bound proteins at PAS- anti TMEM126A/OXA1L columns were eluted by adding 0.1 M glycine, pH 2.8 at room temperature (RT).

### Cross-linking experiments

Mitochondria from HEK293 cells were isolated and metabolic labeling of newly synthesized mitochondrially encoded genes performed as described previously.<sup>58</sup> Briefly, isolated mitochondria were resuspended at 1mg/mL in translation buffer (25 mM HEPES, 100mM mannitol, 80 mM KCl, 5 mM MgCl<sub>2</sub>, 10 mM sodium succinate, 1 mM potassium phosphate, 5 mM ATP, 6 mM creatine phosphate, 0.625 mg/mL creatine kinase, 1 mg/mL BSA, 0.02 mM GTP, 0.15mM amino acid mix (minus methionine), 100 µg/mL emetine, pH 7.4). Samples were incubated for 5 min at 37°C, 100 µCi/mL of [<sup>35</sup>S] methionine was added, and the translation was performed for 25 minutes at 37°C with continuous shaking in the presents of 1mM of SPDP crosslinker. As a control, an equal volume of DMSO was added to another sample. The crosslinking reaction was quenched with 50 mM Tris/HCL pH 7.4 buffer. Mitochondria were then pelleted down at 11,000g at 4°C for 10min and washed with phosphate-buffered saline (PBS). Mitochondrial pellets were further used for TMEM126A immunoprecipitation. Mitochondria were resuspended in 100 µl of SDS solubilization buffer (50mM Tris/HCL, 150mM NaCl, 10mM MgCl<sub>2</sub>, 10% Glycerol, 1% SDS, 1% Triton X-100, 1X protease inhibitor (EDTA free)-Thermo scientific, 1mM PMSF) and incubate for 15 min at room temperature. SDS and Triton X-100 were diluted to 900µl in the same buffer without detergents. Debris was removed at 11,000g at 4°C for 10 min. TMEM126A antibody crosslinked agarose beads were added to the supernatant and incubated at 4°C or 1 hour. Beads were then washed with wash buffer (50mM Tris/HCL, 150mM NaCl, 10mM MgCl<sub>2</sub>, 10% Glycerol, 1% Digitonin, 1X protease inhibitor (EDTA free)-Thermo scientific, 1mM PMSF). For elution, 1M glycine pH 2.8 buffer was sued at 100xg for 1 min and loaded on T4-12% tris glycine gel.

### Blue-Native-PAGE/ 2D-SDS-PAGE analysis

Protein complexes were separated using Blue Native-polyacrylamide gel electrophoresis (BN-PAGE) as described before.<sup>59</sup> Isolated mitochondria were solubilized in BN-PAGE lysis buffer containing 20mM Tris/HCl (pH7.4), 0.1 M EDTA, 50 mM NaCl, 10% glycerol, 1 mM PMSF, 0.4% DDM or 1% digitonin with a protein concentration of 1µg/µl and incubated for 20 min. After centrifugation at 16,000 x g, 4°C lysates were mixed with 10 x BN-PAGE sample buffer (0.5% Coomassie Brilliant Blue G-259, 50 mM 6-aminocaproic acid, 10 mM Bis-Tris, pH 7.0) and loaded on a 4-13% or 2.5-10% gradient gel. Proteins were either transferred onto PVDF membranes or further subjected to 2D-SDS-PAGE.

### Mass spectrometry

For the analysis of OXA1L and TMEM126A complexes, HEK293 cells expressing FLAG-tagged OXA1L and wild type cells were cultured in SILAC medium containing stable isotope-coded 'heavy' L-arginine and L-lysine (<sup>13</sup>C<sub>6</sub><sup>15</sup>N<sub>x</sub>; Cambridge Isotope Laboratories) or the unlabeled 'light' counterparts. Protein complexes were isolated from mitochondrial fractions, OXA1L complexes via the FLAG tag and TMEM126A complexes via antibody immunoprecipitation as described above (n = 4 each, including a label switch). To analyze the effect of TMEM126A knockout on the mitochondrial proteome, equal amounts of crude mitochondrial fractions obtained from differentially SILAC labeled HEK293 wild type and TMEM126A<sup>-/-</sup> cells were mixed (n = 3 with label-switch). All samples were analyzed by liquid chromatography-mass spectrometry using a Q Exactive Plus mass spectrometer (Thermo Fisher Scientific, Bremen, Germany). Proteins were identified using MaxQuant/Andromeda (version 1.6.0.1 for the analysis of OXA1L complexes and version 2.2.0.0 for the analysis of TMEM126A complexes) and mitochondrial fractions from TMEM126A<sup>-/-</sup> versus wild type cells,<sup>60,61</sup> with default settings and the UniProt human ProteomSet including isoforms. Protein abundance ratios were log<sub>2</sub>-transformed, mean log<sub>2</sub> ratios were calculated, and p-values were determined using a two-sided Student's t-test. Ratios reported for OXA1L complexes (Table S1) are based on ratios provided by MaxQuant. For the determination of ratios reported for TMEM126A complexes (Table S2) and TMEM126A knockout experiments (Table S3), log<sub>2</sub>-transformed MaxQuant normalized ratios were further processed using the cyclic loess approach<sup>62</sup> followed by imputation of missing values<sup>63</sup> or proteins quantified in only 2/3 replicates (TMEM126A knockout data) or 3/4 replicates (TMEM126A complexes), respectively.

### QUANTIFICATION AND STATISTICAL ANALYSIS

Quantitative statistical analyses are presented as error bars ± standard error of the mean (SEM) or as graphs for the mass spectrometry analyses. The presented number of repeats (n) describes the number of individual biological replicates. Blots or autoradiography quantifications were performed using ImageQuant software, provided by Cytiva. Statistical analyses of mass spectrometry was performed by MaxQuant/Andromeda (version 1.6.0.1 for the analysis of OXA1L complexes and version 2.2.0.0 for the analysis of TMEM126A complexes) as described in the [methods details](#) section. The number of performed biological repeats (n) for each experiment is stated in the figure legends.